Technical Report

TR-10-41

Thermo-mechanical cementation effects in bentonite investigated by unconfined compression tests

Ann Dueck, Clay Technology AB

January 2010

Svensk Kärnbränslehantering AB
Swedish Nuclear Fuel
and Waste Management Co

Box 250, SE-101 24 Stockholm
Phone +46 8 459 84 00

ISSN 1404-0344
SKB TR-10-41

Thermo-mechanical cementation effects in bentonite investigated by unconfined compression tests

Ann Dueck, Clay Technology AB

January 2010

Keywords: Bentonite, Unconfined compression test, Reduced strain at failure.

Abstract

Results from the project LOT /Karnland et al. 2009/ showed that specimens exposed to warm conditions had a significantly reduced strain at failure compared to reference material. The objective of the present study was to investigate the impact of parameters such as temperature, density, water content and degree of saturation on the occurrence of brittleness at failure of bentonite specimens.

To quantify the influence of the different parameters the unconfined compression test was used on specimens with a height and diameter of 20 mm. In this test the relation between stress and strain is determined from axial compression of a cylindrical specimen.

Brittle failure is in this investigation mainly seen on specimens having a density of $\rho \geq 2{,}060$ kg/m^3 or on specimens exposed to high temperature $T \geq 150$°C in the laboratory. Brittle failure behaviour was also seen on unsaturated specimens with a degree of saturation less than $S_r < 90\%$. Failure at reduced strain was seen in this investigation on specimens exposed to $T = 150$°C, on specimens having a water content of $w_i = 0\%$ before saturation, on specimens with a final degree of saturation of $S_r \leq 97\%$ and also on one specimen subjected to consolidation during preparation.

Brittle failure and reduced strain were noticed in the heated field exposed material in the LOT project. Similar behaviour was also observed in the present short term laboratory tests. However, the specimens in the present study showing this behaviour had higher density, lower degree of saturation or were exposed to higher temperatures than the field exposed specimens.

Sammanfattning

Resultat från projektet LOT /Karnland et al. 2009/ visade att prover som utsatts för varma förhållanden i fält uppvisade signifikant minskade töjningar vid brott jämfört med referensmaterialet. Syftet med den aktuella studien har varit att undersöka betydelsen av parametrar som till exempel temperatur, densitet, vattenkvot och vattenmättnadsgrad för bentonitprovers sprödhet vid brott.

För att kvantifiera inverkan av olika parametrar har enaxliga tryckförsök utförts på prover med dimensionerna höjd och diameter lika med 20 mm. Från denna typ av försök kan relationen mellan spänning och töjning bestämmas utifrån axiell belastning av en cylindrisk provkropp.

Sprött brott har i denna undersökning huvudsakligen observerats på prover med en densitet motsvarande $\rho \geq 2\ 060$ kg/m^3 eller på prover som utsatts för höga temperaturer $T \geq 150$ °C i laboratoriet. Sprött brott har också iakttagits på omättade prover med en vattenmättnadsgrad lägre än $S_r < 90\%$. Brott vid reducerad töjning har observerats på prover som utsatts för $T = 150$ °C, på prover med vattenkvot $w_i = 0$ % före vattenmättnad, på prover med slutlig vattenmättnadsgrad $S_r \leq 97$ % och även på ett prov som utsatts för konsolidering under prepareringen.

Sprött brott eller reducerad töjning vid brott observerades på prover som exponerats för varma fältförhållanden i projektet LOT. Liknande uppförande har observerats i de aktuella laboratorieförsöken. Proverna i den aktuella studien där detta uppförande observerades hade dock högre densitet, lägre vattenmättnadsgrad eller hade exponerats för högre temperatur än de fältexponerade proverna.

Contents

1 Introduction

1.1 Background

Mechanical properties such as shear strength are important parameters required by models used for predicting the physical behaviour of saturated buffer in the final disposal of spent nuclear fuel /Börgesson et al. 1995/. The LOT project /Karnland et al. 2009/ provided an opportunity to compare such mechanical properties of buffer material exposed to field conditions relative to the initial properties of reference buffer material. Unconfined compression tests were used to determine the relation between stress and strain.

The results showed that specimens exposed to warm field conditions had a significantly reduced strain at failure compared to reference material. In addition some of the specimens exposed to the most extreme conditions developed a failure surface that deviated from the failure surface which is common in this type of material.

1.2 Objective

The objective with the present study was to investigate the impact of parameters as temperature, stress, strain, density, water content, degree of saturation, gypsum content and dominating exchangeable ions on the failure behaviour and the occurrence of brittleness at failure. In addition the following possible experimental artefacts were studied; initial conditions and friction during shearing. To quantify the influence the unconfined compression test was used.

In this project the word cementation is used as a general term for the process involving a change in mechanical properties including brittleness at failure.

1.3 Unconfined compression tests in the LOT project

An example of the test results from the LOT project /Karnland et al. 2009/ is shown in Figure 1-1. The Figure shows results from the parcel material as deviator stress versus strain and the colours refer to the temperature coupled to the position of the specimens in the LOT parcel. From the warmest to the coldest the colours red, orange, yellow, green, blue and purple represent the average temperatures 125, 115, 100, 90, 40 and 20°C, respectively. The density of each specimen is shown to the right in the diagram. The black lines refer to results from reference material.

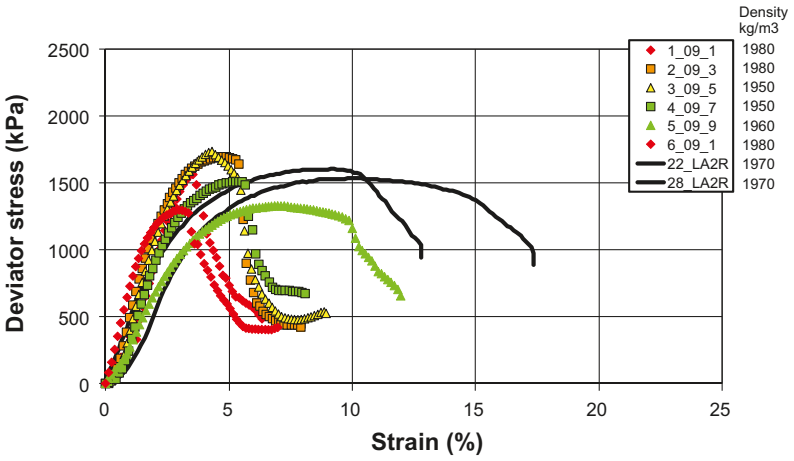

Figure 1-1. *Deviator stress versus strain resulting from unconfined compression tests on material from the LOT project /Karnland et al. 2009/.*

The maximum deviator stress (q_{max}) and the corresponding strain (ε) plotted versus density for the field exposed specimens are shown in Figure 1-2. The open circles were the reference tests linked with a solid best fit line.

The most important conclusions from the project concerning the results from the unconfined compression tests were that in the material from the warm section significantly reduced strain at failure was measured and that a qualitatively different course of shearing involving a more pronounced failure was noticed. Test series with material not exposed to field conditions but heated in a laboratory oven showed a correlation between lower strain at failure and increasing temperature despite the short exposure time in the laboratory oven.

The results and the conclusions from the LOT project was the origin of the present study why also the methodology used was kept in the present study.

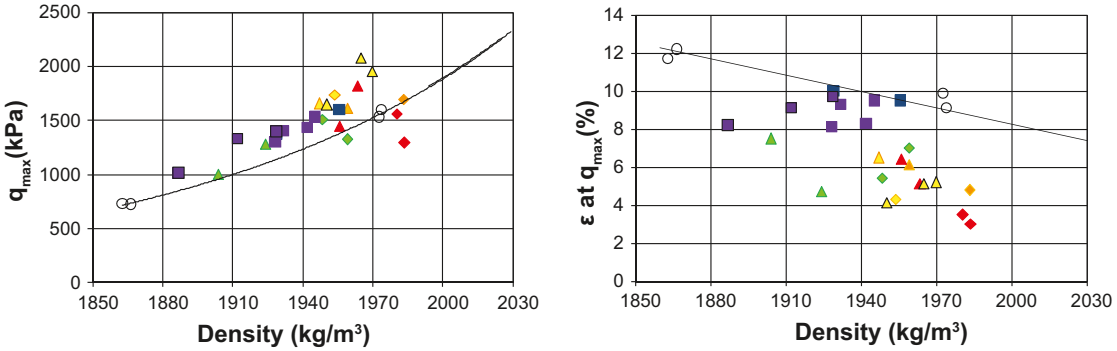

Figure 1-2. *Maximum deviator stress and corresponding strain plotted versus density from unconfined compression tests carried out in the LOT project /Karnland et al. 2009/.*

2 Determination of base variables

2.1 General

The base variables include water content w (%), void ratio e and degree of saturation S_r (%) and were determined according to Equation 2-1–Equation 2-3.

$$w = 100 \cdot \frac{m_{tot} - m_s}{m_s} \quad \text{2-1}$$

$$e = \frac{\rho_s}{\rho}(1 + w/100) - 1 \quad \text{2-2}$$

$$S_r = \frac{\rho_s \cdot w}{\rho_w \cdot e} \quad \text{2-3}$$

where

m_{tot} = total mass of the specimen (g)

m_s = dry mass of the specimen (g)

ρ_s = particle density (kg/m^3)

ρ_w = density of water (kg/m^3)

ρ = bulk density of the specimen (kg/m^3)

The dry mass of the specimen was obtained from drying the wet specimen at 105°C for 24h. The bulk density was calculated from the total mass of the specimen and the volume determined by weighing the specimen above and submerged into paraffin oil.

3 Unconfined compression test

3.1 General

The unconfined compression test has been used in several studies where the mechanical or physical properties of bentonite were of interest. For example has the test been used for evaluating relative physical changes between different positions in the field exposed material and the reference material by /Karnland et al. 2009/. The test has also been used for evaluating effects of different test techniques and effects of material composition by /Dueck et al. 2010/. Another example is the study on influence of shear rate reported by /Börgesson et al. 2004/.

The unconfined compression test is an experimentally simple method where a specimen is compressed axially with a constant rate of strain and no radial confinement or external radial stress. Cylindrical samples are used and the dimensions of the specimen are often a height which is double the size of the diameter. However, in the present study the height of the specimens has been equal to the diameter of the specimens and below is a description of the methodology used.

3.2 Equipment

The specimens were saturated in a special designed device before the shear test. The shearing was made by a mechanical press and a set up shown in Figure 3-1. During the test the deformation and the applied force were measured by means of standard load cell and deformation transducer. All transducers were calibrated prior to the shearing of one series and checked afterwards.

3.3 Preparation of specimen

The specimens were prepared in a compaction device from powder to cylindrical specimens, 20 mm in diameter and 20 mm in height. The specimens were saturated with de-ionized water applied after evacuating the steel filters and tubes in the saturation device. After saturation over a two-week period the specimens were removed from the saturation device at least 12h before the shearing. In two series, A and L, the shearing was carried out directly after the removal from the saturation device. The specimens used in series K and M were not saturated in the saturation device.

Some specimens were prepared from large blocks by drilling and trimming cylindrical specimens, 20 mm in diameter and 20 mm in height. Some of these were saturated in the saturation device.

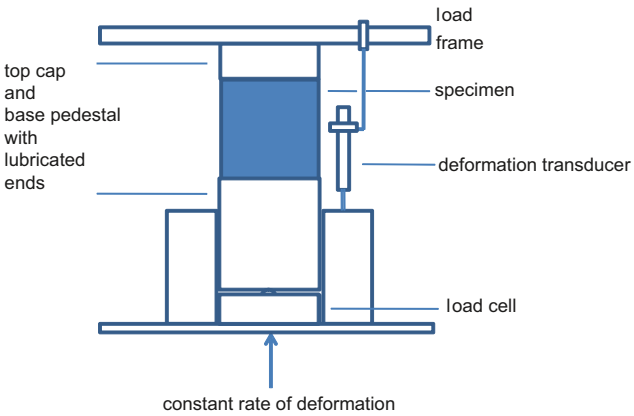

Figure 3-1. *Set-up for the unconfined compression test.*

3.4 Test procedure

The specimens were placed in the mechanical press and the compression started and continued at a constant deformation rate of 0.16 mm/min (or 0.003 mm/s). To minimize boundary effects from the top and bottom during shearing the specimen's ends were lubricated by use of vacuum grease. During shearing the specimens were surrounded by a protective plastic sheet to prevent or minimize evaporation. After failure the water content and density were determined according to Chapter 2.

The heated specimens were, still inside the saturation device, exposed to the maximum temperature during 24h. The increase and decrease in temperature were made in steps of approximately 40°C and each temperature was kept for a minimum of 1h. In one of the series some specimens were only exposed to the maximum temperature during 5h. In series with heated specimens a water pressure was applied to all specimens during the saturation and heating. After the heating the water pressure was reduced to zero for 12h, before the removal from the saturation device. The water pressures 700 kPa and 2,000 kPa were used for specimens exposed to $T = 150$°C and $T = 200$°C, respectively.

3.5 Test results

The specimens were considered as undrained during shearing and no volume change was taken into account. The deviator stress q (kPa) and the strain ε (%) were derived from Equation 3-1 and Equation 3-2, respectively.

$$q = \frac{F}{A_0} \cdot \left(\frac{l_0 - \Delta l}{l_0}\right) \qquad 3\text{-}1$$

$$\varepsilon = \frac{\Delta l}{l_0} \qquad 3\text{-}2$$

where

F = applied vertical load (kN)
A_0 = original cross section area (m^2)
l_0 = original length (m)
Δl = change in length (m)

Initial problems with the contact surface were corrected for. This was done by decreasing the strain with the intercept on the x-axis of a tangent to the stress-strain curve taken at 500 kPa. The new starting point is illustrated in Figure 3-2.

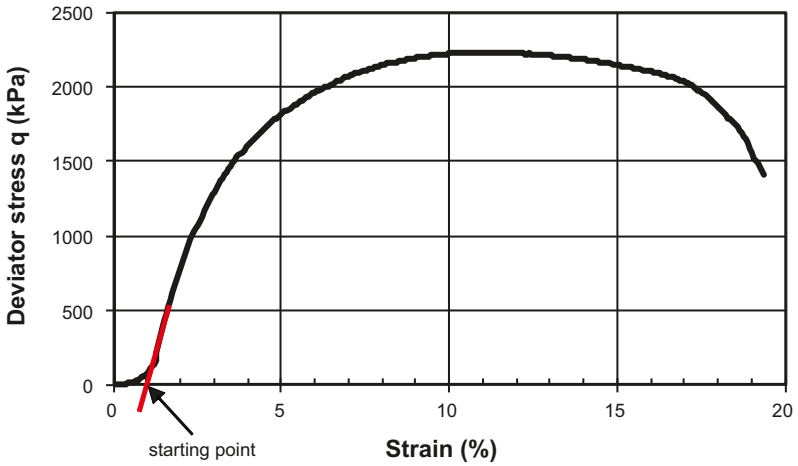

Figure 3-2. *Illustration of the starting point after correction for initial problem with the contact surface.*

4 Materials and test series

4.1 General

Altogether 15 test series were carried through. The series were labelled series A to O. The letters are kept throughout the report. In this chapter each series is mentioned with the material and preparation used and the purpose of each series. The special treatment necessary to meet the mentioned purpose of a series is described with the results from the current series, in section 5.2. The influence is quantified by measurement of stresses and strains during the unconfined compression test described in general terms in Chapter 3.

4.2 Materials used

Four types of bentonite were used in the series; MX-80, Deponit CaN and purified bentonite, WyNa and WyCa.

Properties regarding mineralogy and sealing properties of the sodium dominated MX-80 and the calcium dominated Deponit CaN are reported by /Karnland et al. 2006/. In this report the purified WyNa and WyCa are also mentioned which are ion exchanged MX-80 with all accessory minerals removed.

For the determination of void ratio and degree of saturation the particle density ρ_s = 2,780 kg/m^3 and water density ρ_w = 1,000 kg/m^3 were used for MX-80. For all other materials ρ_s = 2,750 kg/m^3 and water density ρ_w = 1,000 kg/m^3 were used.

4.3 Test series

The material and preparation of the specimens and the purpose of each series are shown in Table 4-1 and Table 4-2, respectively.

Table 4-1. Material and preparation of the specimens in each series.

Series	Material	Preparation	Saturated with solution	Temperature °C
A	MX-80	compacted	de-ionized	20
B	MX-80	compacted	de-ionized	20
C	MX-80	compacted	de-ionized	150
D	MX-80	compacted	de-ionized	20
E	DepCaN	compacted	de-ionized	150, 20
F	MX-80	compacted	de-ionized	200, 20
G	WyNa, WyCa	compacted	de-ionized	150, 20
H	MX-80	compacted	de-ionized	20
I	MX-80	drilled	de-ionized	80–110
J	MX-80	milled and re-compacted	de-ionized	80–110
K	MX-80	drilled	–	80–110
L	MX-80	compacted	de-ionized	20
M	MX-80	compacted	–	20
N	MX-80, DepCaN	compacted	de-ionized	–18
O	MX-80	compacted	de-ionized	150, 20

Table 4-2. Purpose of each series and the number of specimens used.

Series	The purpose of the series was to study	Number of specimens
A	influence of swelling and initial stresses of MX-80	6
B	influence of different preparation of MX-80	10
C	influence of time of exposure of MX-80 to 150°C	6
D	influence of initial water content of MX-80	10
E	DepCaN exposed to 150°C	6
F	MX-80 exposed to 200°C	6
G	purified WyNa and WyCa exposed to 150°C	6
H	influence of water content at compaction of MX-80	10
I	MX-80 field exposed to 80–110°C	3
J	MX-80 field exposed to 80–110°C	3
K	effect of stress anisotropy of MX-80	6
L	effect of stress path of MX-80	2
M	effect of degree of saturation of MX-80	16
N	influence of freezing of MX-80 and DepCaN	10
O	influence of gypsum content in MX-80	6

5 Results

5.1 General

All test series carried out in this project are presented in separate sections below. Each section starts with a brief description of the objective of the test series and details regarding deviations from the preparation and test procedure presented in Chapter 3. Each section ends with the test results presented as a graph and in tabular form.

Each test is denoted by a letter A–O, representing the test series, and a serial number. This notation is used in the legends of each graph together with values of characteristic variables as maximum temperature, density or initial water content, e.g. *C107 150 1900* denoting *test number_maximum temperature (°C)_density (kg/m³)*. The notations are described in the captions of each graph. The density ρ used in this chapter is the bulk density.

The tests were numbered according to the following. Tests 100–136 were carried out in test series with 6 specimens and tests 200–240 were carried out in series with 10 specimens. The series I to L were numbered differently. Tests I01–I03 and J01–03 were carried out together with a total of 6 specimens. None of the specimens in test series K and M were saturated in the saturation device. The tests in series K were numbered K01–K06 and in series M the first two figures represent the water content and the third represents a serial number.

5.2 Results of test series A–O

A. Influence of swelling and initial stresses of MX-80

Three specimens were compacted into the saturation device introducing high initial radial stresses and then saturated under almost constant volume conditions. Three specimens were compacted to a volume less than the available volume in the saturation device and the consequently swelling, approximately 15%, took place during the saturation. The time between removal from the saturation device and shearing was minimized.

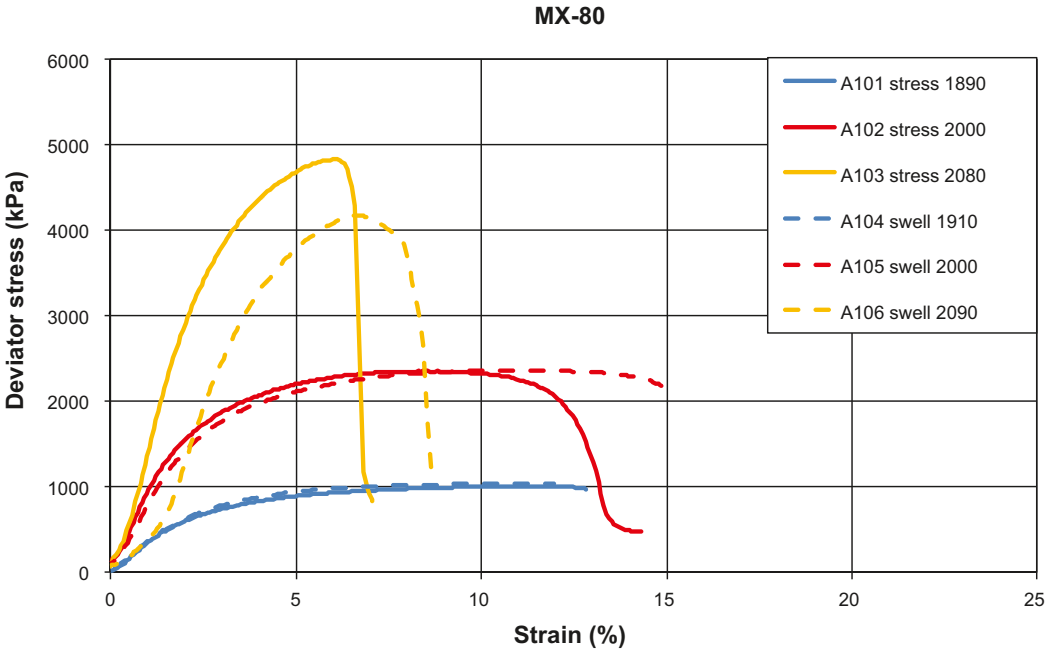

Figure 5-1. *Series A. The legend shows the initial condition, initial stress (stress) or over-compaction (swell) and the density (kg/m³).*

Table 5-1. Test series A.

Test ID	Material	Final values			At shearing		Max T	Remarks
		ρ	w	S_r	Max q	ε		
		kg/m³	%	%	kPa	%	°C	
A101	MX-80	1,890	36.0	100	1,000	11.1	room	no swelling
A102	MX-80	2,000	28.4	101	2,350	8.5	room	no swelling
A103	MX-80	2,080	23.0	99	4,830	6.0	room	no swelling
A104	MX-80	1,910	35.2	101	1,030	10.3	room	swelling
A105	MX-80	2,000	27.9	100	2,360	10.5	room	swelling
A106	MX-80	2,090	23.1	101	4,170	6.5	room	swelling

B. Influence of different preparation of MX-80

In this series different conditions concerning friction between the specimens and the steel equipment were investigated. In addition the effect of an extra effort to make the end surfaces plane parallel and the effect of 12h delay between the removal from the saturation device and the shearing were investigated. Plastic filters, which can be considered as less rigid than the ordinary steel filters, were used in this series.

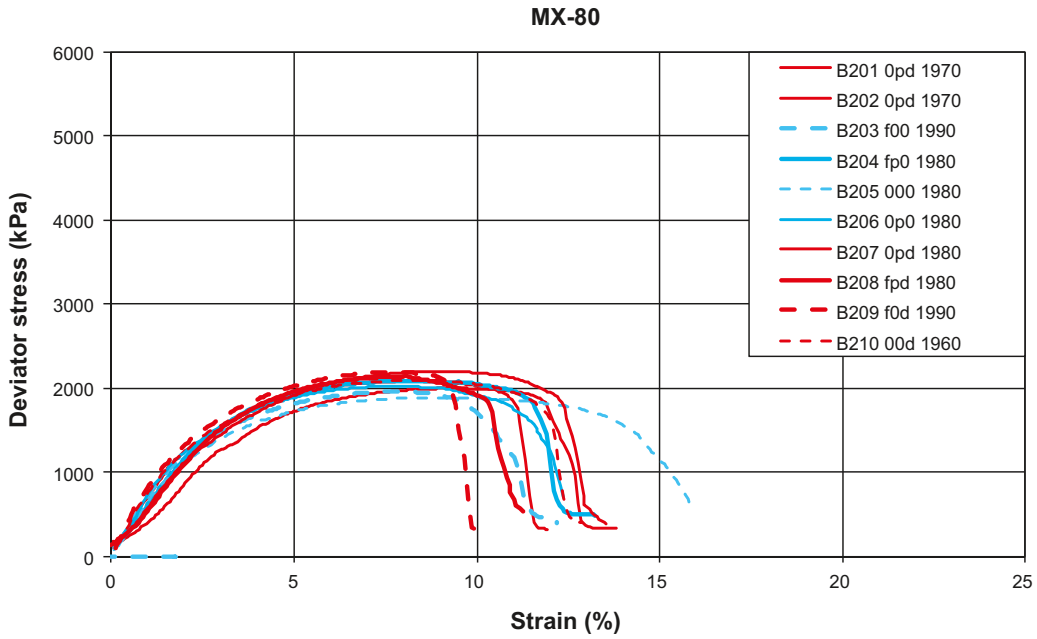

Figure 5-2. *Series B. The legend shows friction on the end surfaces during shear (0 or f), extra effort in making the specimen surfaces plane parallel (0 or p), 12h delay before shear test (0 or d) and density (kg/m³). Details are presented in Table 5-2.*

Table 5-2. Test series B.

Test ID	Material	Final values			At shearing		Max T	Remarks
		ρ	w	S_r	Max q	ε		friction/plane ends/delay
		kg/m³	%	%	kPa	%	°C	
B201	MX-80	1,970	29.3	99	2,000	9.3	room	-/plane/delay
B202	MX-80	1,970	28.8	98	2,080	8.3	room	-/plane/delay
B203	MX-80	1,990	29.9	102	1,950	7.7	room	friction/-/-
B204	MX-80	1,980	29.5	101	2,090	7.9	room	friction/plane/-
B205	MX-80	1,980	29.8	101	1,890	8.7	room	-/-/-
B206	MX-80	1,980	29.6	101	2,020	7.8	room	-/plane/-
B207	MX-80	1,980	29.1	99	2,200	8.9	room	-/plane/delay
B208	MX-80	1,980	28.9	99	2,130	7.6	room	friction/plane/ delay
B209	MX-80	1,990	29.2	101	2,190	7.6	room	friction/-/delay
B210	MX-80	1,960	28.7	96	2,090	8.2	room	-/-/delay

C. Influence of time of exposure of MX-80 to 150°C

In this series the effect of the time of exposure to 150°C was investigated; 5h or 24h.

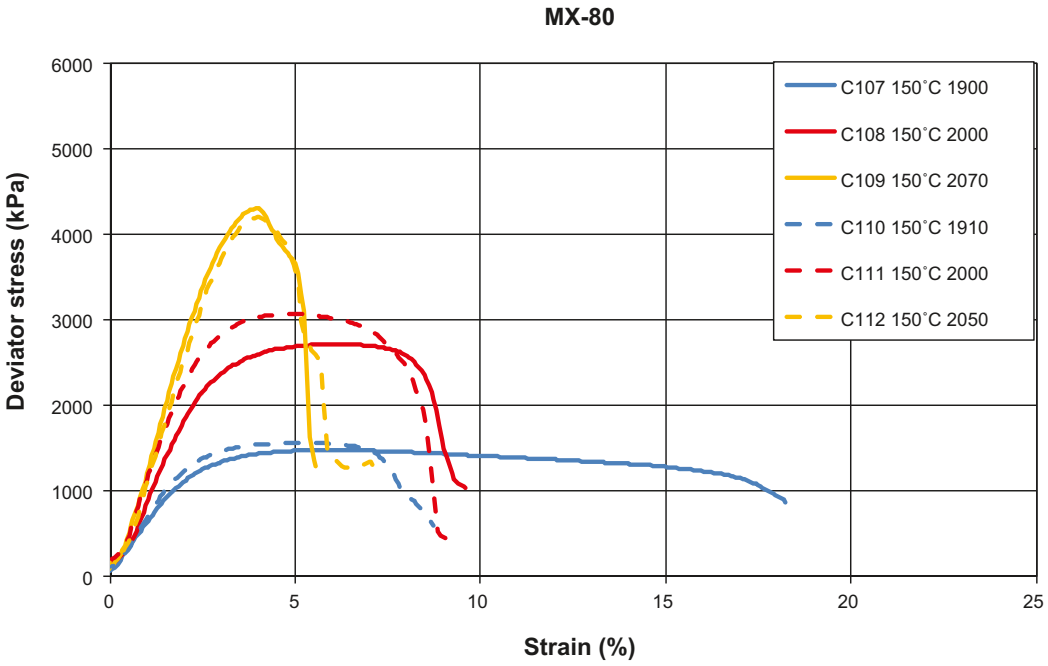

Figure 5-3. *Series C. The legend shows maximum temperature after saturation (°C) and the density (kg/m³). Solid lines denote 5h of exposure and broken lines denote 24h of exposure. Details are presented in Table 5-3.*

Table 5-3. Test series C.

Test ID	Material	Final values			At shearing		Max T	Remarks
		ρ	w	S_r	Max q	ε		
		kg/m³	%	%	kPa	%	°C	
C107	MX-80	1,900	35.0	100	1,470	5.5	150	5h of exposure
C108	MX-80	2,000	28.5	101	2,720	6.0	150	5h of exposure
C109	MX-80	2,070	24.0	100	4,300	3.9	150	5h of exposure
C110	MX-80	1,910	34.8	100	1,560	4.8	150	24h of exposure
C111	MX-80	2,000	28.2	101	3,070	4.7	150	24h of exposure
C112	MX-80	2,050	24.4	99	4,190	3.8	150	24h of exposure

D. Influence of initial water content of MX-80

The effect of the initial water content before saturation w_i (0%, 16%, 20%, 24%, 27%) was investigated in this series. Plastic filters, which can be considered as less rigid than the ordinary steel filters, were used in this series.

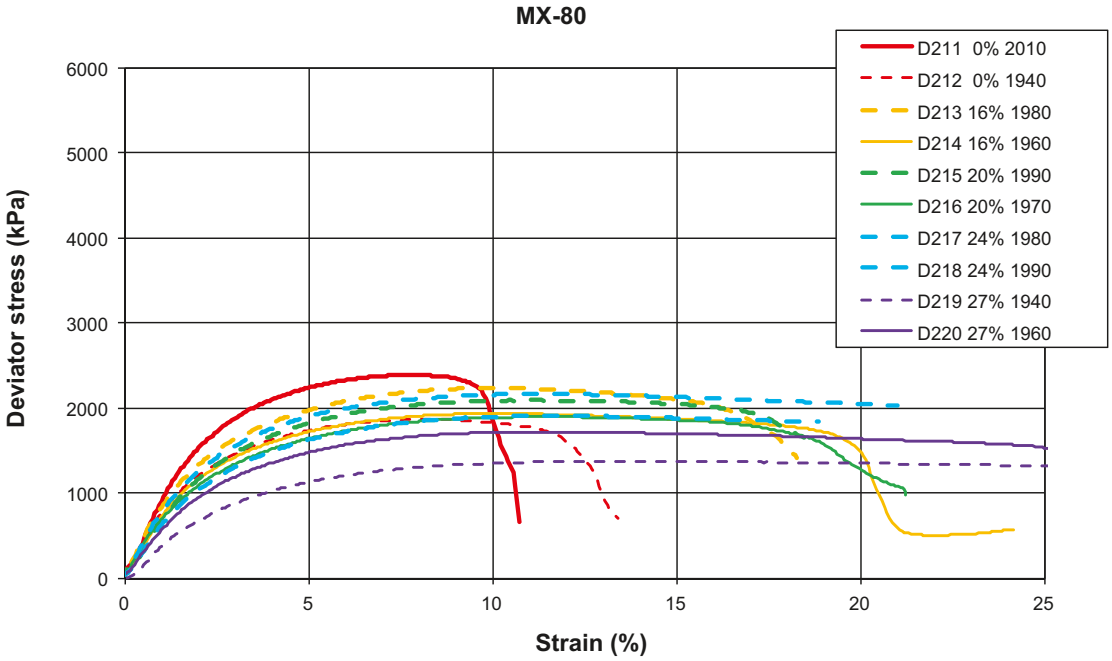

Figure 5-4. *Series D. The legend shows the initial water content and the density (kg/m³). Details are presented in Table 5-4.*

Table 5-4. Test series D.

Test ID	Material	Final values			At shearing		Max T	Remarks
		ρ kg/m³	w %	S_r %	Max q kPa	ε %	°C	initial water content (%)
D211	MX-80	2,010	27.1	99	2,380	7.9	room	0[1]
D212	MX-80	1,940	29.7	97	1,860	7.8	room	0[1]
D213	MX-80	1,980	28.2	98	2,230	9.7	room	16
D214	MX-80	1,960	29.4	98	1,930	9.8	room	16
D215	MX-80	1,990	28.1	99	2,090	11.1	room	20
D216	MX-80	1,970	29.9	100	1,890	11.1	room	20
D217	MX-80	1,980	29.2	100	1,900	11.1	room	24
D218	MX-80	1,990	28.1	99	2,160	11.3	room	24
D219	MX-80	1,940	31.9	100	1,370	12.9	room	27
D220	MX-80	1,960	30.4	100	1,720	11.1	room	27

[1] compacted at w = 10%.

E. DepCaN exposed to 150°C

In this series three specimens of Deponit CaN were exposed to 150°C and three reference specimens were placed at room temperature.

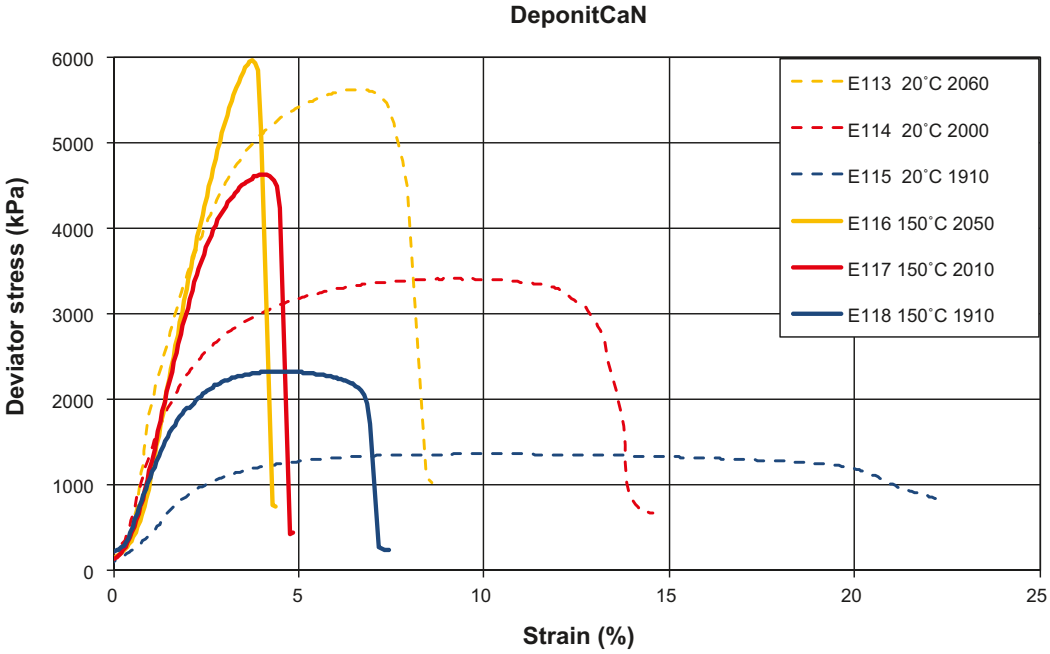

Figure 5-5. *Series E. The legend shows maximum temperature after saturation (°C) and the density (kg/m³). Details are presented in Table 5-5.*

Table 5-5. Test series E.

Test ID	Material	Final values			At shearing		Max T	Remarks
		ρ	w	S_r	Max q	ε		
		kg/m³	%	%	kPa	%	°C	
E113	DepCaN	2,060	24.5	102	5,620	6.5	20	
E114	DepCaN	2,000	27.7	101	3,410	8.8	20	
E115	DepCaN	1,910	35.1	102	1,360	9.6	20	
E116	DepCaN	2,050	25.2	102	5,950	3.7	150	
E117	DepCaN	2,010	27.5	101	4,630	4.0	150	
E118	DepCaN	1,910	34.0	101	2,320	4.3	150	

F. MX-80 exposed to 200°C

In this series three specimens of MX-80 were exposed to 200°C during 24h and three reference specimens were placed at room temperature.

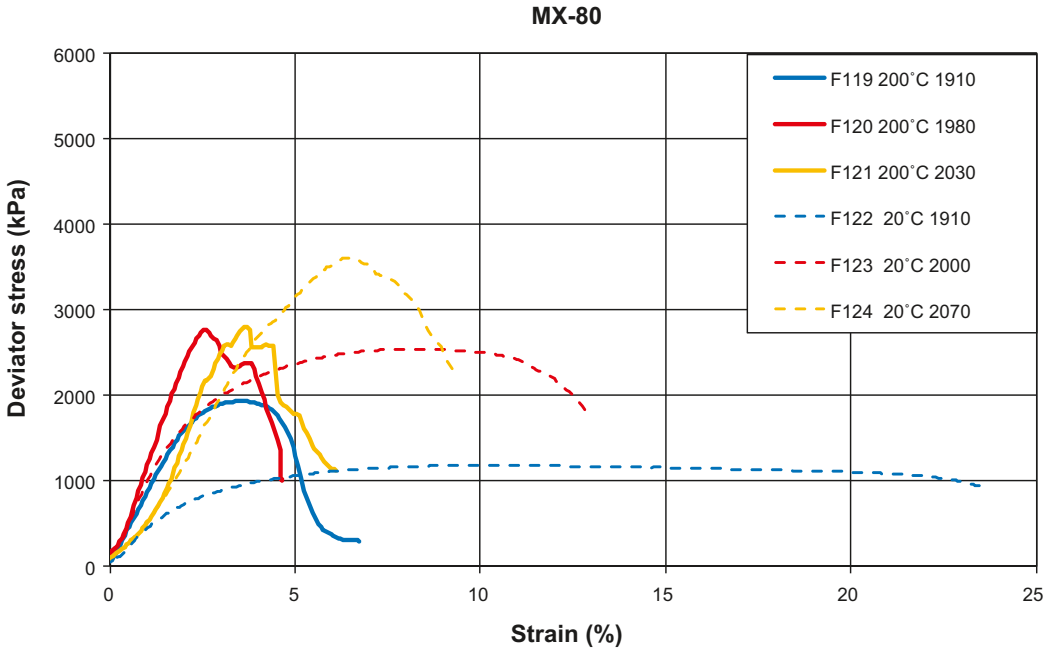

Figure 5-6. *Series F. The legend shows the maximum temperature after saturation (°C) and the density (kg/m³). Details are presented in Table 5-6.*

Table 5-6. Test series F.

Test ID	Material	Final values			At shearing		Max T	Remarks
		ρ	w	S_r	Max q	ε		
		kg/m³	%	%	kPa	%	°C	
F119	MX-80	1,910	35.3	101	1,930	3.4	200	
F120	MX-80	1,980	28.9	99	2,760	2.5	200	
F121	MX-80	2,030	24.8	98	2,790	3.6	200	
F122	MX-80	1,910	34.6	100	1,180	9.8	20	
F123	MX-80	2,000	27.3	99	2,540	8.0	20	
F124	MX-80	2,070	22.1	96	3,610	6.4	20	

G. Purified WyNa and WyCa exposed to 150°C

In this series, purified WyNa and WyCa were used. The dominating exchangeable ions in those materials are sodium and calcium, respectively. These purified materials were ion exchanged from MX-80 as described by /Karnland et al. 2006/ and all accessory minerals were removed. Some of the specimens were exposed to 150°C some were placed at room temperature. The specimen G128 had a horizontal fracture already at removal from the saturation device, i.e. before shearing. It was tested in spite of this.

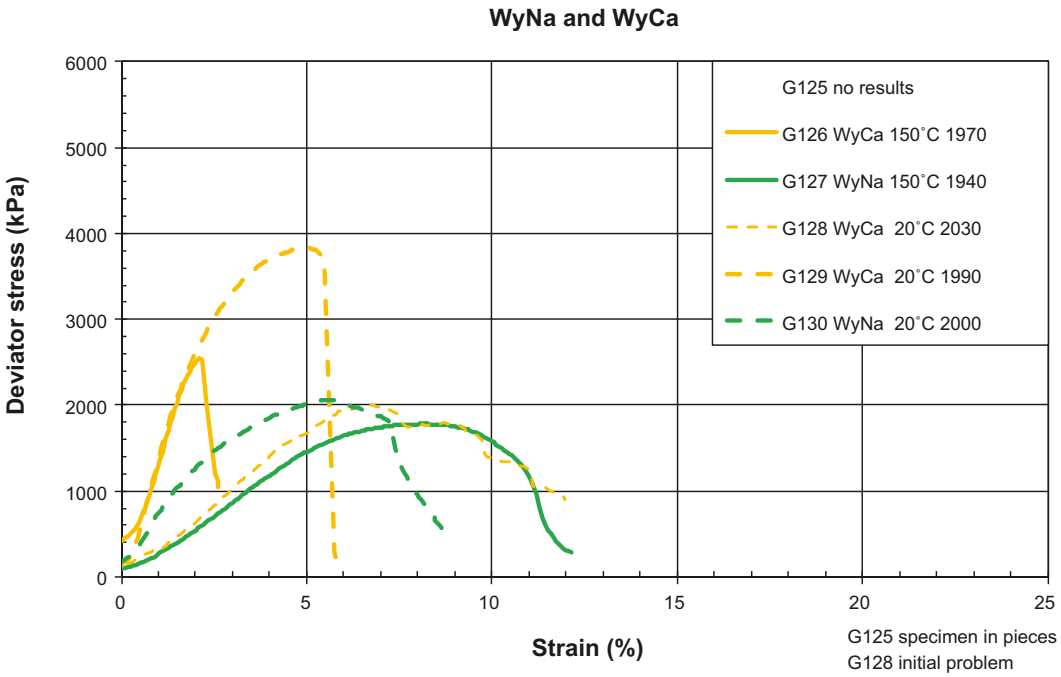

Figure 5-7. *Series G. The legend shows the material, the maximum temperature after saturation (°C) and the density (kg/m³). Details are presented in Table 5-7.*

Table 5-7. Test series G.

Test ID	Material	Final values			At shearing		Max T	Remarks
		ρ	w	S_r	Max q	ε		
		kg/m³	%	%	kPa	%	°C	
G125	WyCa		27.5				150	no results
G126	WyCa	1,970	29.5	101	2,540	2.1	150	
G127	WyNa	1,940	30.9	99	1,780	8.2	150	
G128	WyCa	2,030	25.7	101	2,010	6.7	20	initial problems
G129	WyCa	1,990	27.3	99	3,830	4.8	20	
G130	WyNa	2,000	28.6	102	2,060	5.6	20	

H. Influence of water content at compaction of MX-80

In this series the influence of different initial water content before saturation (0%, 10%, 27%) was investigated. In addition different water contents at compaction were used. The pair of water contents (w_c and w_i) 10% and 0% denote that this specimen was compacted at w_c = 10% and then dried to w_i = 0% just before saturation.

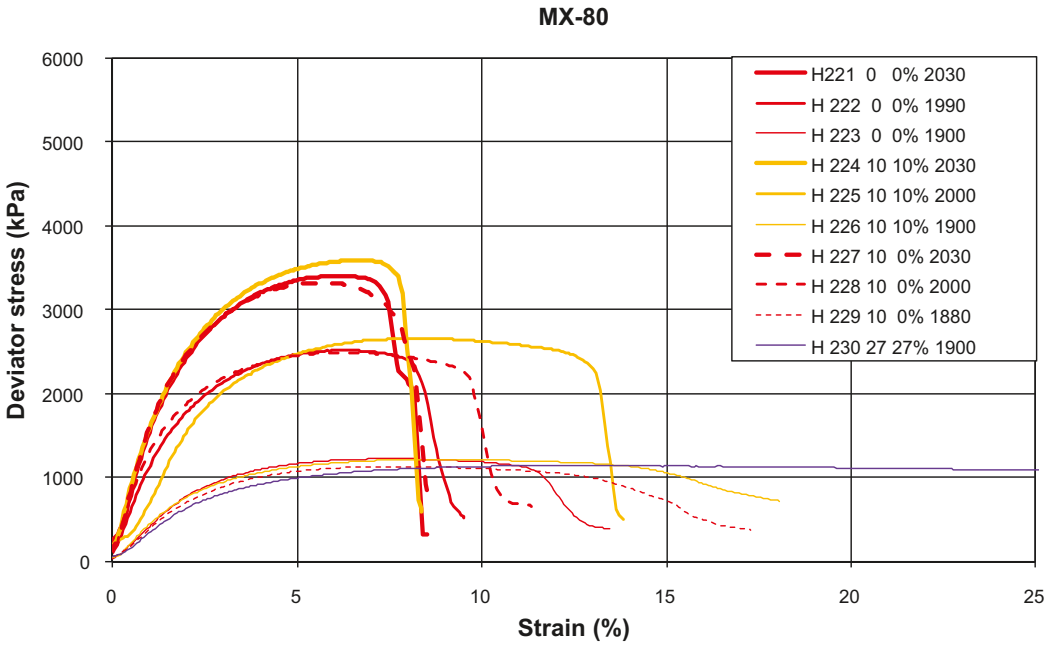

Figure 5-8. *Series H. The legend shows the water content (%) at compaction and the water content (%) at the start of the saturation and finally the density (kg/m³). Details are presented in Table 5-8.*

Table 5-8. Test series H.

Test ID	Material	Final values			At shearing		Max T	Remarks water contents w_c, w_i (%)[1]
		ρ	w	S_r	Max q	ε		
		kg/m³	%	%	kPa	%	°C	
H221	MX-80	2,030	24.9	98	3,400	6.0	room	0 0
H222	MX-80	1,990	27.5	98	2,510	6.1	room	0 0
H223	MX-80	1,900	34.2	99	1,220	7.3	room	0 0
H224	MX-80	2,030	25.0	98	3,580	6.4	room	10 10
H225	MX-80	2,000	27.7	99	2,650	8.2	room	10 10
H226	MX-80	1,900	34.3	98	1,210	8.8	room	10 10
H227	MX-80	2,030	24.7	97	3,320	5.7	room	10 0
H228	MX-80	2,000	27.7	99	2,480	5.9	room	10 0
H229	MX-80	1,880	34.4	97	1,130	7.6	room	10 0
H230	MX-80	1,900	34.9	100	1,140	11.7	room	27 27

[1] w_c – water content at compaction, w_i water content at start saturation.

IJ. MX-80 field exposed to 80–110°C

Field material from the ABM project /Eng et al. 2007/ was used in this series. Three specimens (I01–I03) were drilled and re-saturated in the saturation device. Three specimens (J01–J03) were drilled, milled, re-compacted and re-saturated in the saturation device. The temperatures are preliminary and not yet published and the approximate time of exposure was 1 year. This limited test series will be followed by more tests which will later be reported with other laboratory tests on field exposed material and field data from the ABM project.

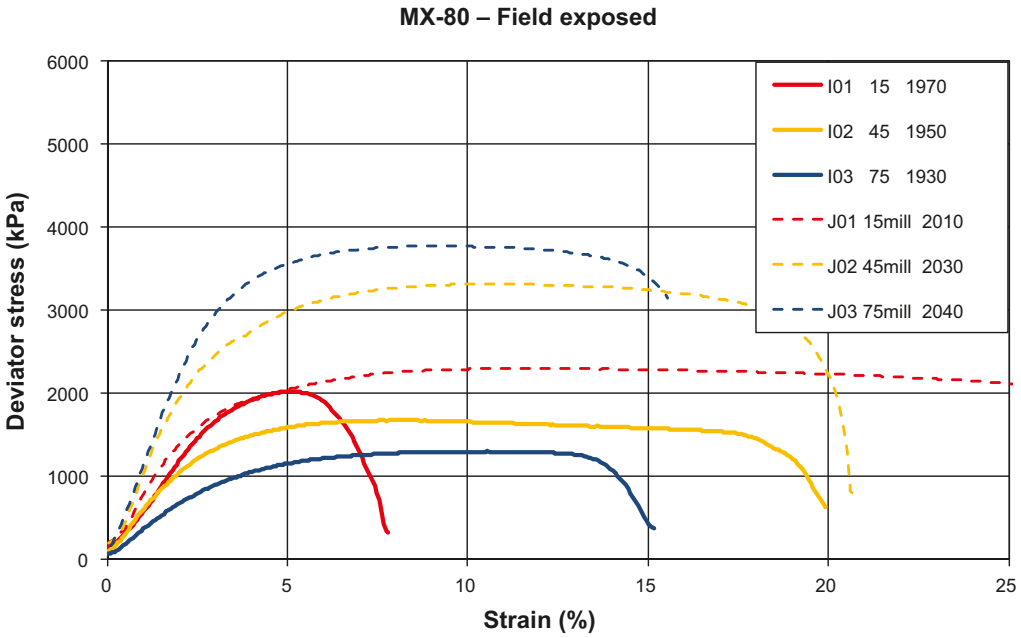

Figure 5-9. *Series IJ. The legend shows distance (mm) from heater where each specimen was taken and the density (kg/m³). Specimens milled and re-compacted are marked with mill after the distance (e.g. 15mill). Details are presented in Table 5-9.*

Table 5-9. Test series IJ.

Test ID	Material	Final values			At shearing		Max T	Remarks field exposed material
		ρ	w	S_r	Max q	ε		
		kg/m³	%	%	kPa	%	°C	
I01	MX-80	1,970	29.7	99	2,020	5.1	110[1]	drilled
I02	MX-80	1,950	30.8	99	1,670	7.8	90[1]	drilled
I03	MX-80	1,930	33.4	100	1,300	9.4	80[1]	drilled
J01	MX-80	2,010	26.8	98	2,300	11.7	110[1]	milled and re-compacted
J02	MX-80	2,030	24.7	97	3,310	10.3	90[1]	milled and re-compacted
J03	MX-80	2,040	24.2	97	3,770	8.8	80[1]	milled and re-compacted

[1] Max T from block 27, material from block 29. Approximate values.

K. Effect of stress anisotropy of MX-80

The effect of anisotropy was investigated by shearing specimens vertically or horizontally drilled from a field exposed block from the ABM project /Eng et al. 2007/. The specimens in this series were not re-saturated in the saturation device.

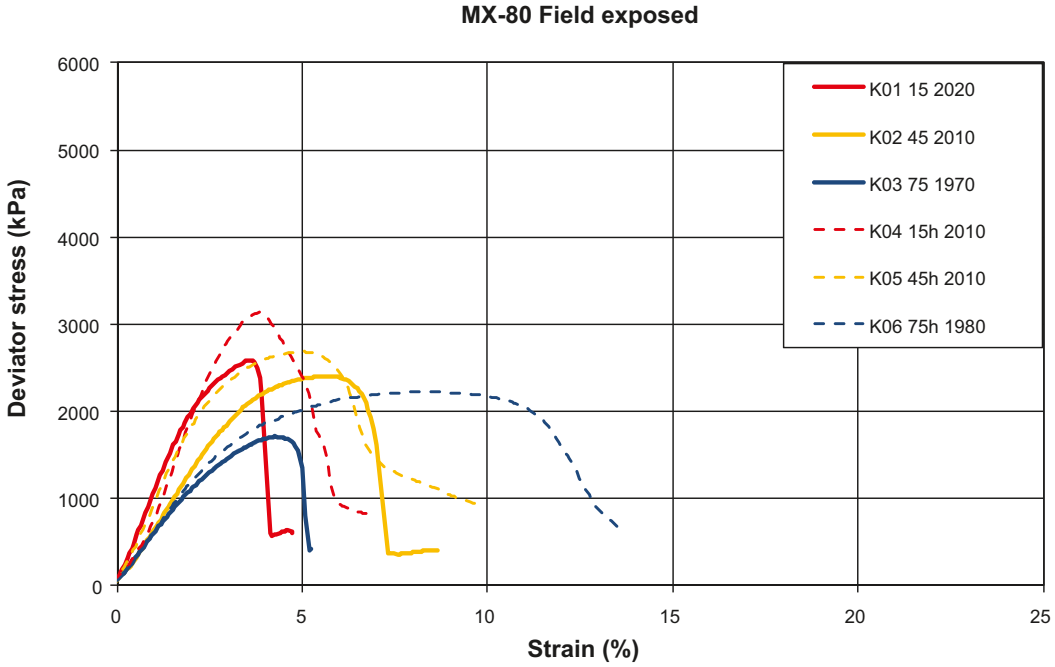

Figure 5-10. *Series K. The legend shows distance from the heater where each specimen was taken and the density (kg/m³). None of the specimens in this series were saturated in the saturation device. Specimens drilled horizontally are marked with h (e.g. 15h) which deviates from the usual vertical drilling. Details are presented in Table 5-10.*

Table 5-10. Test series K.

Test ID	Material	Final values			At shearing		Max T	Remarks field exposed material, no saturation
		ρ	w	S_r	Max q	ε		
		kg/m³	%	%	kPa	%	°C	
K01	MX-80	2,020	26.4	99	2,590	3.5	110[1]	drilled vertical
K02	MX-80	2,010	26.6	98	2,400	5.6	90[1]	drilled vertical
K03	MX-80	1,970	28.1	97	1,710	4.2	80[1]	drilled vertical
K04	MX-80	2,010	26.3	98	3,130	3.8	110[1]	drilled horizontal
K05	MX-80	2,010	26.9	99	2,690	5.0	90[1]	drilled horizontal
K06	MX-80	1,980	28.8	99	2,230	8.5	80[1]	drilled horizontal

[1] Max T from block 27, material from block 29. Approximate values.

L. Effect of stress path of MX-80

This series consists of two specimens and the ordinary saturation device was not used for the saturation. The specimen L1a was consolidated in steps from a low density and a height of 24.5 mm to a height of 20 mm. The specimen L1b was allowed to swell in steps from a high density and a height of 18.5 mm to a height of 20 mm. The initial mass of the two specimens were equal and the intention was to end up with two specimens that have experienced different stress paths but with the same final density. The stress paths and the deformation for each specimen are shown in detail in Appendix 1. The time between removal from the saturation device and shearing was minimized.

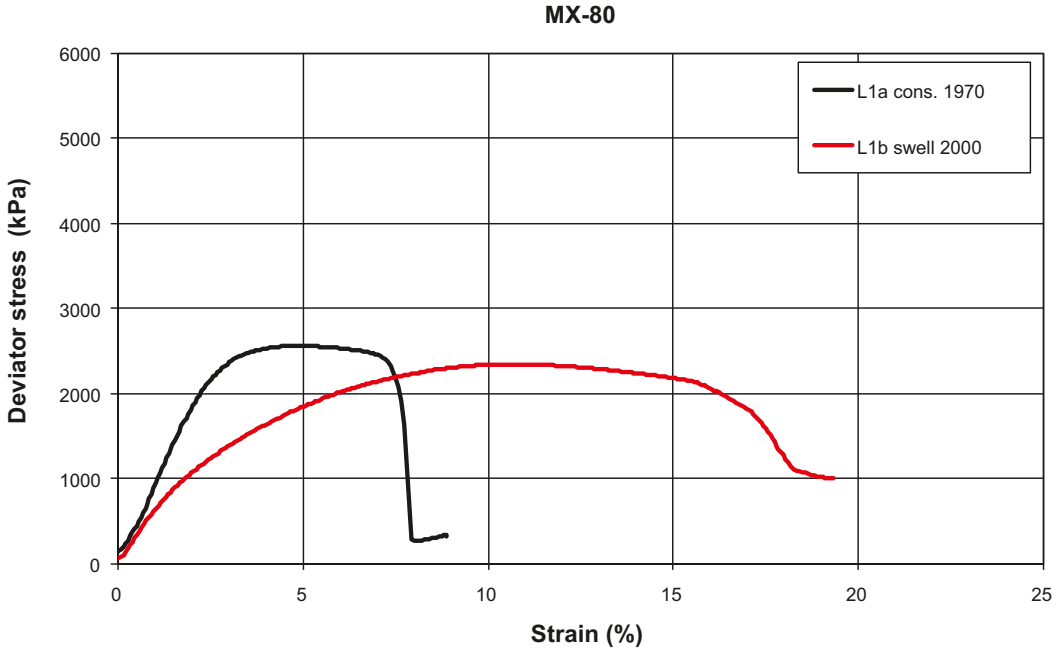

Figure 5-11. *Series L. The legend shows the condition during preparation and the density (kg/m³). During preparation one specimen was allowed to consolidate (cons.) from a low density and one specimen was allowed to swell (swell) from a high density. Details are presented in Table 5-11.*

Table 5-11. Test series L.

Test ID	Material	Final values			At shearing		Max T	Remarks
		ρ	w	S_r	Max q	ε		
		kg/m³	%	%	kPa	%	°C	
L1a	MX-80	1,970	30.2	100	2,560	4.7	room	consolidated
L1b	MX-80	2,000	28.4	100	2,340	10.7	room	swelled

M. Effect of degree of saturation of MX-80

In this series the influence of degree of saturation was investigated. The specimens were compacted from powder with different initial water contents and compaction pressures. The specimens in this series were not saturated in the saturation device. In Figure 5-12 the colours (red, yellow, dark blue, light blue) denote the ranges of density (2,050–2,110, 2,000–2,040, 1,950–1,990, 1,900–1,940 kg/m^3) and the line styles (▬ , ── , ╌ ╌ , ·····) denote the ranges of degree of saturation (98–100%, 90–97%, 80–89%, 70–79%).

The deviator stress has been evaluated according to Equation 3-1 even though the volume change might deviate from zero since these specimens were unsaturated. This test series was performed by Lars Ohlsson.

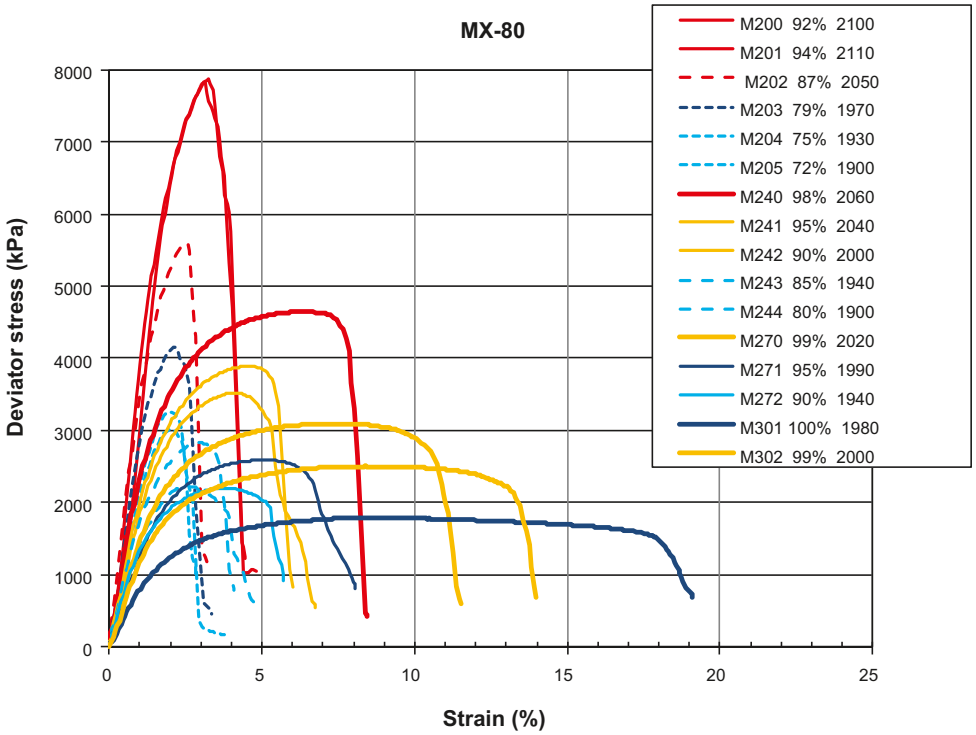

Figure 5-12. *Series M. The legend shows the degree of saturation (%) and the density (kg/m³). None of the specimens were saturated in the saturation device. Details are presented in Table 5-12.*

Table 5-12. Test series M.

Test ID	Material	Final values			At shearing		Max T	Remarks
		ρ	w	S_r	Max q	ε		
		kg/m³	%	%	kPa	%	°C	
M200	MX-80	2,100	19.4	92	7,870	3.2	room	no saturation
M201	MX-80	2,110	19.4	94	7,820	3.1	room	no saturation
M202	MX-80	2,050	19.5	87	5,610	2.5	room	–
M203	MX-80	1,970	19.3	79	4,160	2.1	room	–
M204	MX-80	1,930	19.4	75	3,260	2.0	room	–
M205	MX-80	1,900	19.5	72	3,010	2.0	room	–
M240	MX-80	2,060	23.3	98	4,640	6.3	room	–
M241	MX-80	2,040	23.3	95	3,890	4.6	room	–
M242	MX-80	2,000	23.2	90	3,520	4.1	room	–
M243	MX-80	1,940	23.1	85	2,830	3.0	room	–
M244	MX-80	1,900	23.1	80	2,230	2.5	room	–
M270	MX-80	2,020	25.9	99	3,100	7.4	room	–
M271	MX-80	1,990	25.9	95	2,600	5.0	room	–
M272	MX-80	1,940	25.8	90	2,200	3.7	room	–
M301	MX-80	1,980	29.3	100	1,790	8.3	room	–
M302	MX-80	2,000	27.4	99	2,510	8.3	room	no saturation

N. Influence of freezing of MX-80 and DepCaN

All specimens in this series were put in the freezer at –18°C after saturation and still inside the saturation device, i.e. at constant volume conditions. In Figure 5-13 the colours green and yellow denote MX-80 and Deponit CaN, respectively.

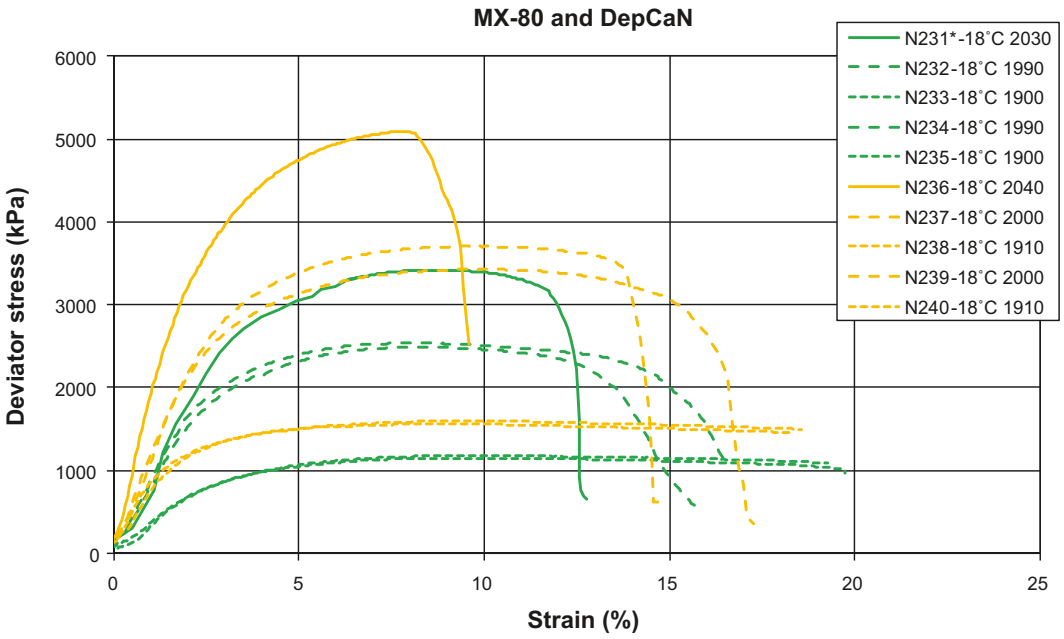

Figure 5-13. *Series N. The legend shows minimum temperature after saturation (°C) and the density (kg/m³). Details are presented in Table 5-13. N231* were measured from a screen plot. The colours green and yellow denote MX-80 and Deponit CaN, respectively.*

Table 5-13. Test series N.

Test ID	Material	Final values			At shearing		Min T	Remarks
		ρ	w	S_r	Max q	ε		
		kg/m³	%	%	kPa	%	°C	
N231	MX-80	2,030	25.7	99	3,420	9.0	–18	
N232	MX-80	1,990	28.3	99	2,540	8.0	–18	
N233	MX-80	1,900	35.2	100	1,150	9.2	–18	
N234	MX-80	1,990	28.9	100	2,490	8.0	–18	
N235	MX-80	1,900	35.3	100	1,180	9.6	–18	
N236	DepCaN	2,040	24.7	99	5,090	7.9	–18	
N237	DepCaN	2,000	27.8	101	3,420	9.4	–18	
N238	DepCaN	1,910	34.0	101	1,600	9.4	–18	
N239	DepCaN	2,000	27.0	100	3,700	9.2	–18	
N240	DepCaN	1,910	33.8	100	1,560	8.4	–18	

O. Influence of gypsum content in MX-80

Different contents of gypsum (CaSO4×2H2O) were mixed with MX-80. The content (0, 2% and 5%) was calculated from the dry weight of the MX-80.

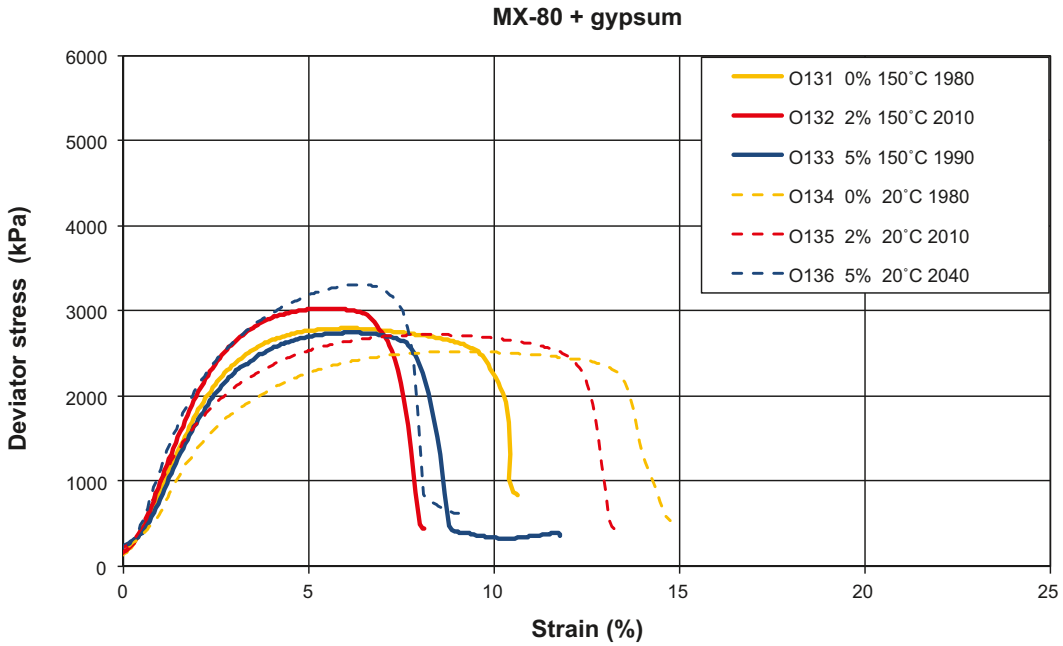

Figure 5-14. *Series O. The legend shows content of gypsum (as % of the dry weight of the bentonite), maximum temperature after saturation (°C) and the density (kg/m³). Details are presented in Table 5-14.*

Table 5-14. Test series O.

Test ID	Material	Final values			At shearing		Max T	Remarks content of gypsum (%)[1]
		ρ	w	S_r	Max q	ε		
		kg/m³	%	%	kPa	%	°C	
O131	MX-80	1,980	28.9	99	2,790	6.0	150	0
O132	MX-80	2,010	28.0	101	3,030	5.4	150	2
O133	MX-80	1,990	27.9	99	2,750	6.1	150	5
O134	MX-80	1,980	27.6	97	2,520	8.8	room	0
O135	MX-80	2,010	27.1	99	2,720	8.0	room	2
O136	MX-80	2,040	25.4	99	3,310	6.5	room	5

[1] Per cent of the dry weight of the bentonite. The dry weight of the bentonite was the same in all specimens.

6 Analysis

6.1 General

The results from the test series are compared to each other and to results from other projects. The following issues are focused on:

1. Impact of preparation – stress path (series A and L).
2. Impact of preparation – initial water content (series D and H).
3. Impact of test technique (series B).
4. Impact of temperature (series C, E, F, N, /Karnland et al. 2009/).
5. Impact of dominating exchangeable ions (series E, F, G, and /Dueck et al. 2010/).
6. Impact of gypsum content (series O).
7. Impact of degree of saturation (series M).
8. Impact of stress anisotropy (series K).
9. Impact of field condition (series I).
10. Impact of milling and re-compaction (series J, /Karnland et al. 2009/).
11. Impact of shear rate (/Dueck et al. 2010/).

In this chapter the results from the test series are presented as maximum deviator stress q_{max} (kPa) and corresponding strain ε (%) both as a function of bulk density ρ (kg/m^3). In all diagrams reference lines, based on the results from the reference tests in the LOT project /Karnland et al. 2009/, are shown and denoted as *reference*. The lines represent MX-80 specimens compacted from water content 10% and prepared and tested according to the standard methodology described in Chapter 3 at room temperature. In Figure 6-1 the reference lines are shown with the test results they were based upon, denoted *LOT series 1*.

The bulk density used in the LOT project was determined from the mass of the specimen and the volume inside the saturation device. In the present study the bulk density was determined after the test according to Chapter 2. Both types of densities are regarded as representative for the bulk density used in this analysis and referred to as the density ρ.

Figure 6-2a shows a specimen with an ordinary shear failure and the corresponding failure surface. In the following the brittleness of failures will be discussed. The term *brittle failure* will here be used for the special case of brittleness when no continuous deformation occurs at the maximum deviator stress and an abrupt decrease in stress is observed in the stress-strain curve after failure. Figure 6-2b shows an example of a *brittle failure* and the corresponding failure surface which is often more or less vertical for this type of failure.

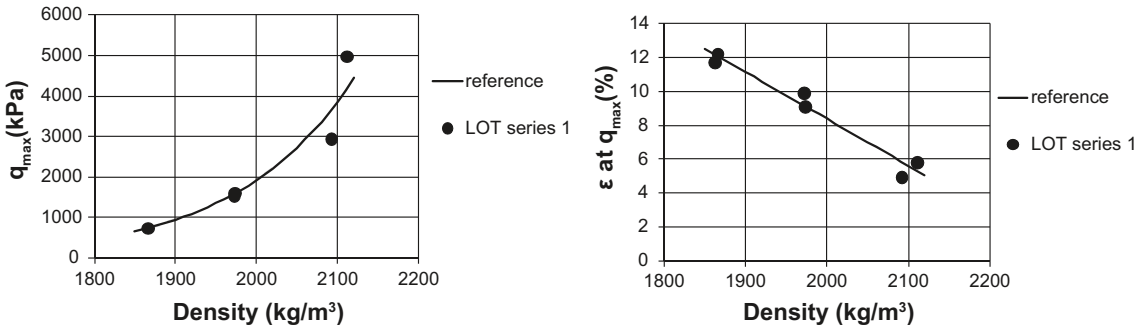

Figure 6-1. *Maximum deviator stress q_{max} and corresponding strain ε vs. density. Also shown are best fit lines (reference) based on the reference tests (LOT series 1) in the LOT project representing MX-80 /Karnland et al. 2009/.*

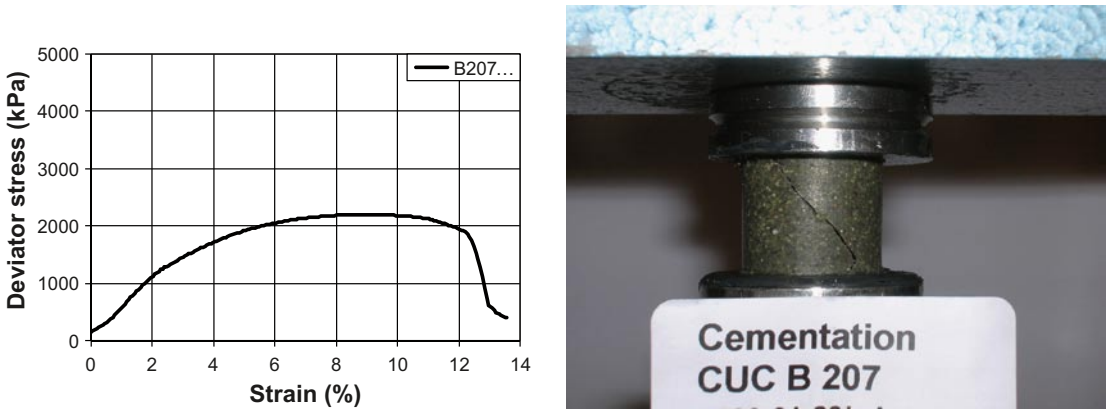

Figure 6-2a. *Example of an ordinary shear failure and the corresponding failure surface.*

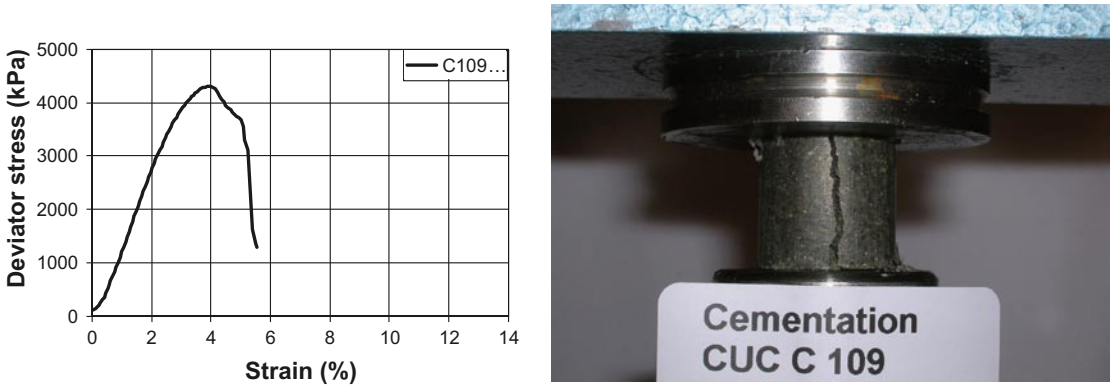

Figure 6-2b. *Example of a brittle failure and the corresponding failure surface.*

6.2 Comparison and determining factors

6.2.1 Impact of preparation – stress path

In Figure 6-3 the impact of different stress paths during preparation is shown. The specimens *A swell* and *L swell* represent specimens where swelling or an increase in volume during saturation was allowed. The specimens *A stress* and *L cons.* were subjected to constant volume and decreased volume respectively, during saturation.

High density specimens of the reference group failed at relatively small strain. This was also the case for the A series. In the L series the specimen exposed to gradual consolidation during saturation (*L cons.*) also failed at relatively small strain in contrast to the specimen exposed to swelling (*L swell*).

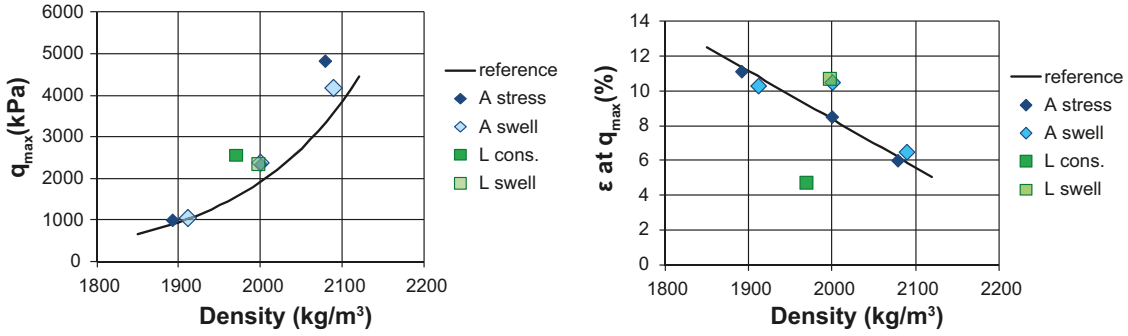

Figure 6-3. *Maximum deviator stress and corresponding strain from series A and L.*

Thus, small strain at failure was seen at high densities or after gradual consolidation. An indication of *brittle failure* was noticed on the high density specimens.

6.2.2 Impact of preparation – initial water content

The results from D and H series, where the specimens were compacted at different initial water contents, are shown in Figure 6-4. In the D series, plastic filters were used instead of the ordinary steel filters which gave slightly less rigid equipment compared to series H. This gave lower final density than predicted in series D. The specimens having high initial water contents were almost compacted to saturation, especially those with an initial water content of $w_i = 27\%$.

The results are also shown as deviator stress vs. strain at four density intervals in Figures 6-5a to 6-5d.

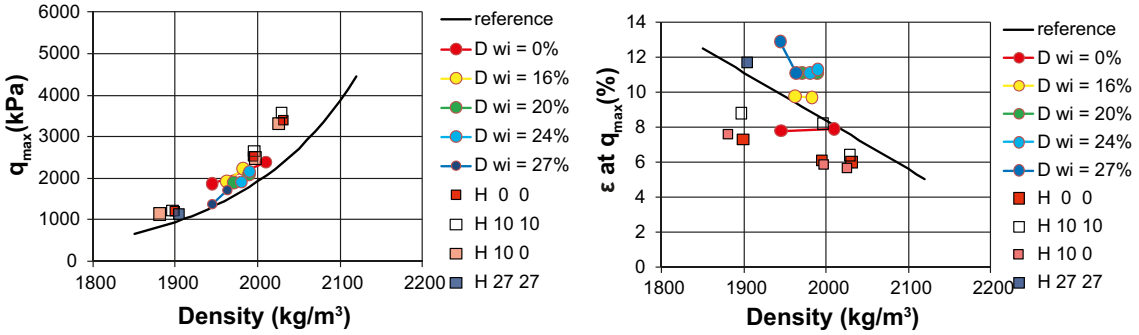

Figure 6-4. *Maximum deviator stress and strain vs. density from series D and H.*

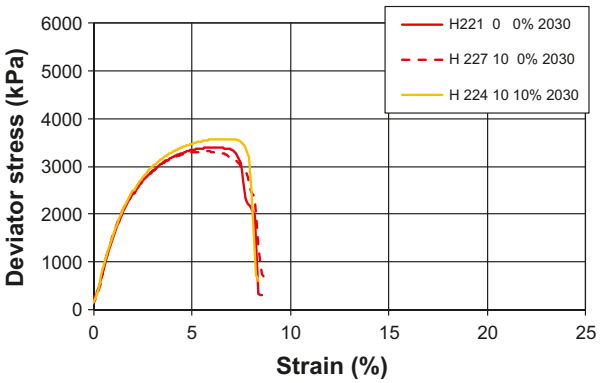

Figure 6-5a. *Influence of initial water content. The material is MX-80 with a density of 2,030 kg/m³.*

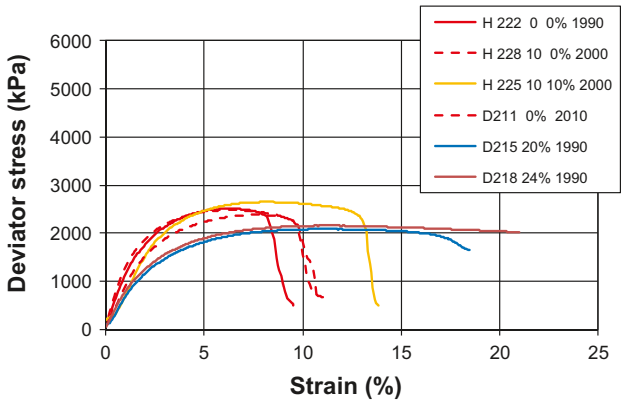

Figure 6-5b. *Influence of initial water content. The material is MX-80 with a density of 1,990–2,010 kg/m³.*

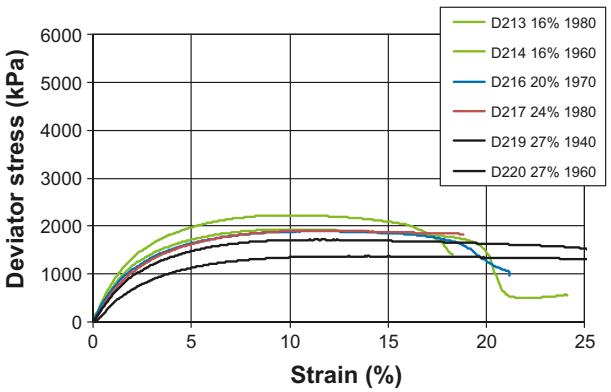

Figure 6-5c. *Influence of initial water content. The material is MX-80 with a density of 1,940–1,980 kg/m³.*

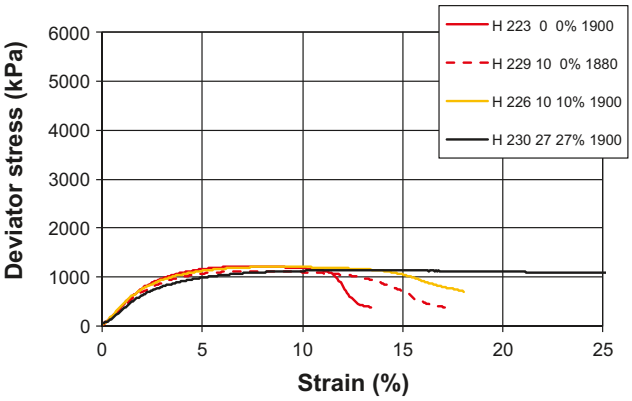

Figure 6-5d. *Influence of initial water content. The material is MX-80 with a density of 1,880–1,900 kg/m³.*

There seems to be an effect of initial water content but only on the strain at failure which increases with increasing initial water content. No significant difference due to different water content at compaction was seen. The more rigid equipment used in series H might have caused less strain in general which probably was a result of the degree of saturation being between 97% and 99% for all specimens but specimen H 27 27 in the series H.

Thus, small strain at failure was seen on specimens having an initial water content of $w_i = 0\%$ independent of the water content at compaction. No indication of *brittle failure* was seen.

6.2.3 Impact of test technique

In test series B impact of friction on the end plates during shearing and impact of time between the removal from the saturation device and shearing were investigated, see Figure 6-6. Approximately the same density was used for all the specimens.

The most influencing factors of those investigated in series B seem to have been friction on the end surfaces and no delay between the removal from the saturation device and shearing which both decreased the strain at failure. However, no large deviation from the reference was seen.

In the present study all specimens except those in series A and L were tested after a delay between the removal from the saturation device and shearing. If the delay was decisive for the strain the small strain at failure at high density seen in Figure 6-3 should have been an effect of no delay. This is however not consistent with other results in the present study.

However, larger strain than expected was seen on specimens in series D where the final density was lower than predicted. In this case it was presumably caused by deformation of the filters or swelling during the removal from the saturation device.

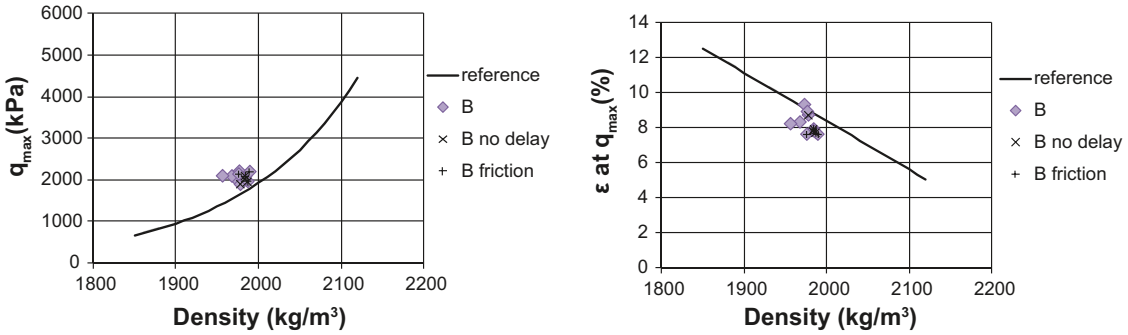

Figure 6-6. *Maximum deviator stress and strain vs. density from series B. All results are marked with lilac coloured diamonds. In addition the results from specimens subjected to friction on the end surfaces and specimens tested immediately, without delay, are marked with pluses and crosses, respectively .*

Thus, the strain at failure was reduced by friction between the specimens and the load frame. In addition, there was an indication that large strain at failure might result from swelling during saturation. No indication of *brittle failure* was seen.

6.2.4 Impact of temperature

Influence of temperature was investigated on both MX-80 and DepCaN at different densities. The results from test series C, E, F and N are shown in Figure 6-7. In Figure 6-8 the results of MX-80 specimens from these series are shown with results from the LOT series 2 with specimens heated in the laboratory /Karnland et al. 2009/. Although reduced strain at failure was seen in the LOT series 2 no brittle failure was seen on these specimens.

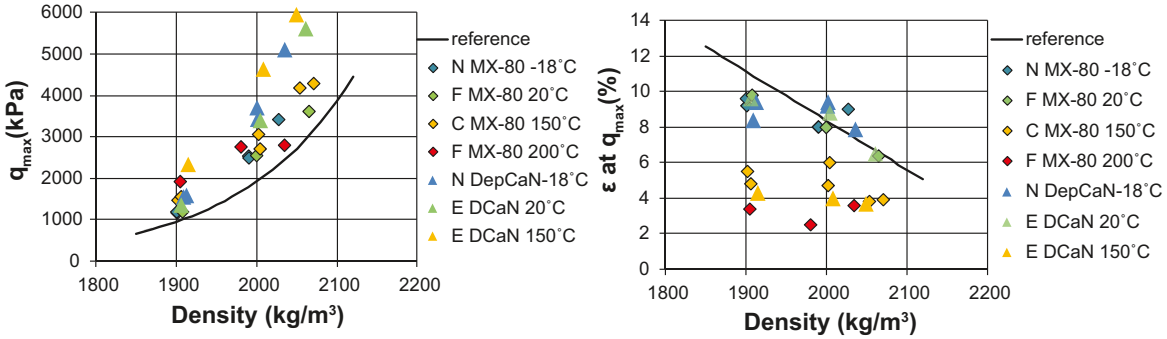

Figure 6-7. *Maximum deviator stress and corresponding strain vs. density from series C, E, F and N with the materials MX-80 and DepCaN.*

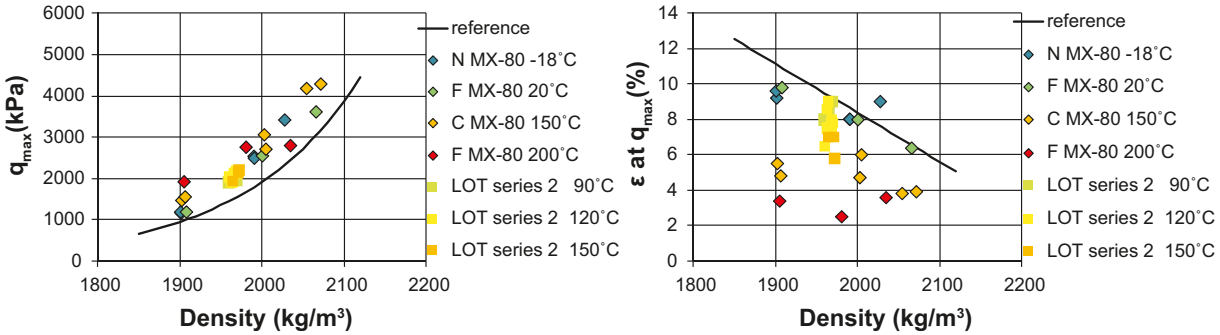

Figure 6-8. *Results from MX-80 specimens from Figure 6-7 with results from LOT series 2 with laboratory heated specimens /Karnland et al. 2009/.*

A tendency towards increasing maximum deviator stress at increasing temperature for MX-80 and DepCaN was seen. Reduced strain at failure was seen at high temperature and the dependence of density on strain, seen at low temperatures, was less at high temperatures. It should be noted that the dependence of density on strain was seen although there was a delay between the removal from the saturation device and the shearing. The results are also shown as deviator stress vs. strain at three density intervals in Figures 6-9a to 6-9c. Examples of brittle failure surfaces from those series are shown in Figures 6-10a, 6-10b and 6-10c.

Thus, a tendency towards increasing maximum deviator stress at increasing temperature was seen. The strain at failure was reduced at increased temperature. Indications that the dependence of density on strain at failure was reduced with increasing temperature were seen. A *brittle failure* was clearly seen on MX-80 specimens at $T = 200°C$ and $\rho = 2{,}030$ kg/m^3. Signs of *brittle failure* was seen on MX-80 and DepCaN specimens already at $T = 150°C$ but then at a higher density of $\rho \approx 2{,}060$ kg/m^3. Small strains at failure were seen at lower temperatures $T \leq 150°C$ on MX-80 specimens in the LOT series 2 with laboratory heated specimens /Karnland et al. 2009/.

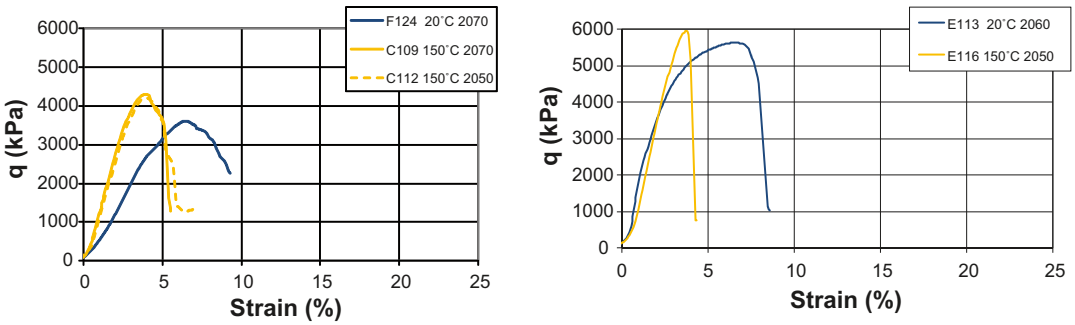

Figure 6-9a. *Influence of temperature on MX-80 (left) and DepCaN (right) with a density about 2,060 kg/m^3.*

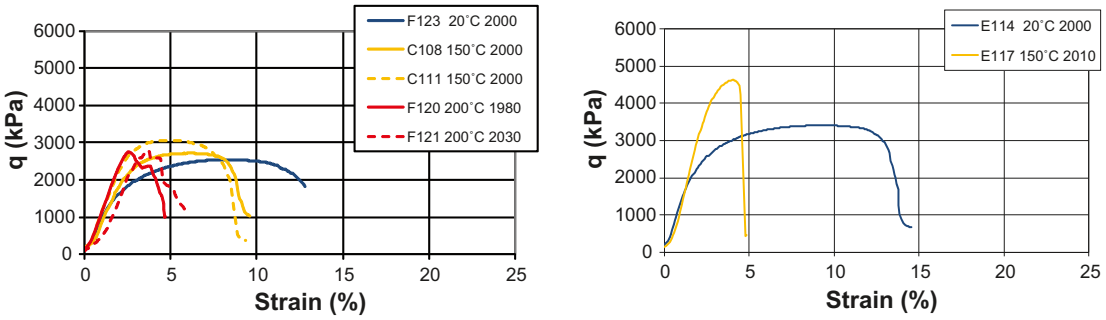

Figure 6-9b. *Influence of temperature on MX-80 (left) and DepCaN (right) with a density about 2,000 kg/m^3.*

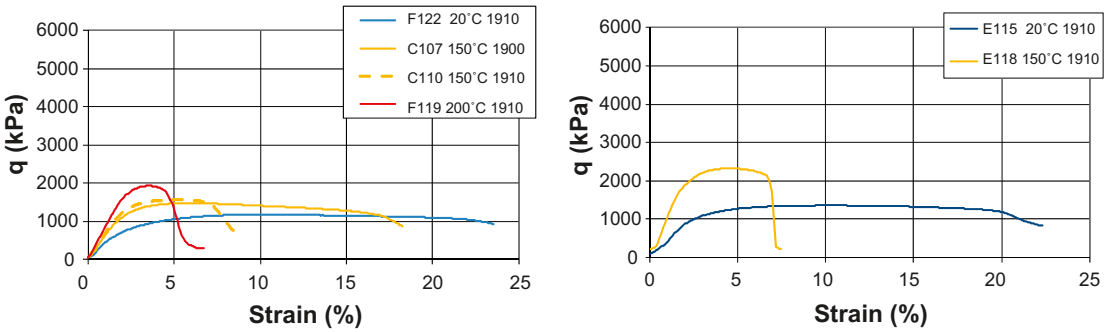

Figure 6-9c. *Influence of temperature on MX-80 (left) and DepCaN (right) with a density about 1,900 kg/m^3.*

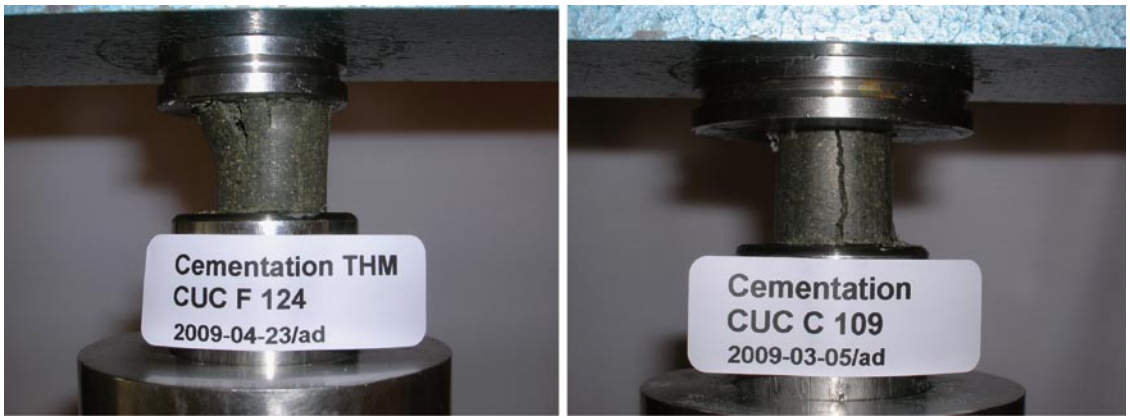

Figure 6-10a. *Failure surfaces of sheared specimens of MX-80 and density of 2,070 kg/m³. The specimens were exposed to room temperature (left) and 150°C (right). (The photo to the right is also shown in Figure 6-2b).*

Figure 6-10b. *Failure surface of sheared specimen of MX-80 and density of 2,030 kg/m³. The specimen was exposed to 200°C.*

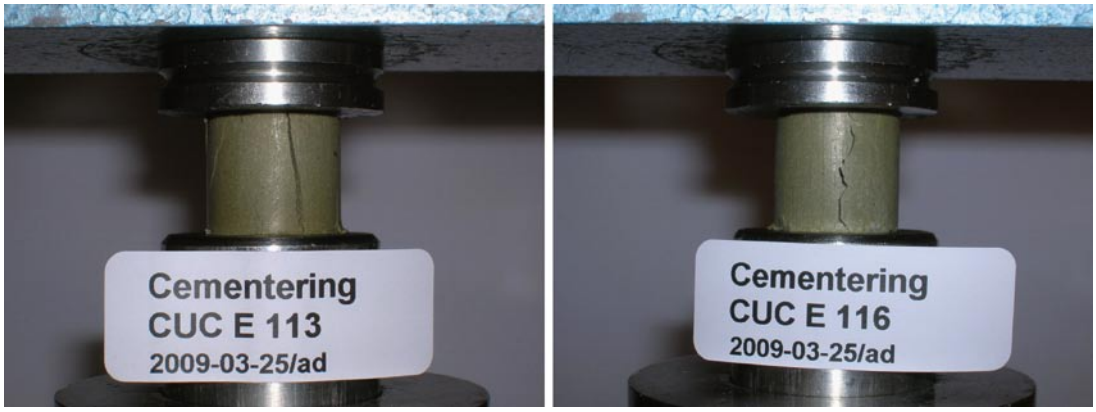

Figure 6-10c. *Failure surfaces of sheared specimens of DepCaN and density 2,050–2,060 kg/m³. The specimens were exposed to room temperature (left) and 150°C (right).*

6.2.5 Impact of dominating exchangeable ions

The difference between results from MX-80 and DepCaN is seen in Figure 6-11. The difference also illustrates the difference between sodium and calcium as dominating exchangeable ions, respectively. In this section the colours (green, yellow) denote the dominating exchangeable ions (sodium, calcium).

In Figure 6-12 the results from the purified bentonites WyNa and WyCa are shown. With an exception of two specimens the tests shown in Figure 6-12 were carried out at room temperature. The two specimens were exposed to 150°C and they are marked with red marker lines in Figure 6-12. There was an initial problem with one of the other specimens which had a horizontal fracture already before shearing, (marked with an arrow). In Figure 6-12 results from /Dueck et al. 2010/ on purified material are also shown (these results have no marker lines).

DepCaN with Ca^{2+} as the dominated ion showed larger maximum deviator stress compared to the Na^{+} dominated MX-80. However, no difference was seen between the two bentonites regarding strain at failure. Indications that the temperature effect is similar in the two bentonites were seen in Figure 6-7.

The purified bentonites differed from the MX-80 and DepCaN specimens in that the strain seems to be larger in WyNa than in WyCa and that the temperature effect on the strain at failure is larger for the WyCa specimen compared to almost no effect for the WyNa specimen. The indication of temperature effect was based on one specimen of WyNa and one of WyCa exposed to 150°C and a vertical failure surface was seen on the heated WyCa specimen.

Thus, almost no difference between MX-80 and DepCaN was seen regarding small strain at failure. Brittle behaviour or reduced strain was seen at high densities on both materials. *Brittle failure* was also seen on specimens of the purified material WyCa.

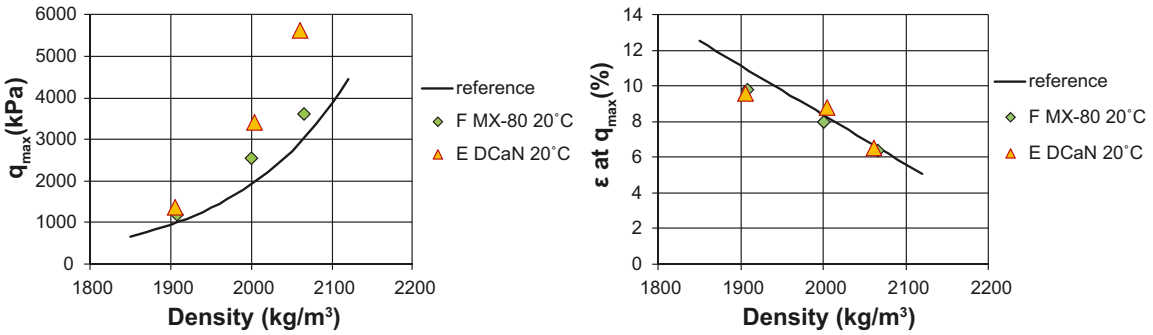

Figure 6-11. *Maximum deviator stress and corresponding strain vs. density for MX-80 and DepCaN at 20°C in series E and F.*

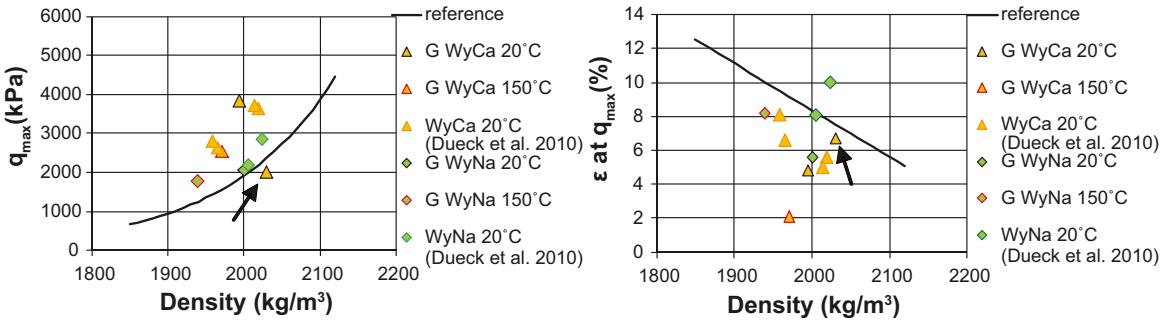

Figure 6-12. *Maximum deviator stress and corresponding strain vs. density for series G. Also shown are results from /Dueck et al. 2010/. There was a problem with the mounting of one specimen, marked with an arrow.*

6.2.6 Impact of gypsum content

In series O the influence of gypsum content was investigated. The results are shown in Figure 6-13. The shapes (diamond, circle, triangle) denote gypsum contents of (0%, 2%, 5%). The colours (green and yellow) denote temperatures (20°C, 150°C).

Content of gypsum does not change the behaviour of the bentonite with temperature. The deviator stress at room temperature corresponds well with previous test results without gypsum. It can be noted that one of the specimens, the green diamond, has a degree of saturation of 97% which might have caused the small deviation from the reference lines. It can also be noted that again the density dependence in strain at failure is seen despite the delay between the removal from the saturation device and the shearing.

Thus, no comments about small strain and *brittle failure* can be made.

6.2.7 Impact of degree of saturation

The influence of degree of saturation is shown in Figure 6-14. The colours (red, yellow, dark blue, light blue) denote intervals of degree of saturation (98–100%, 90–97%, 80–89%, 70–79%, respectively).

For the analysis of influence of degree of saturation on the maximum deviator stress it was more convenient to show the results vs. void ratio which is done in Figure 6-15. When presented like this no influence of degree of saturation was seen on the deviator stress.

However, the degree of saturation seemed to have an important role for the strain at failure. In Figure 6-16 the strain is plotted vs. degree of saturation. The bulk densities are shown as data labels and an influence of density is seen. The black circles represent saturated specimens from the line denoted *reference* in for example Figure 6-14. Photos of the failure surfaces of selected specimens from this series are shown in Figures 6-17a, 6-17b and 6-17c.

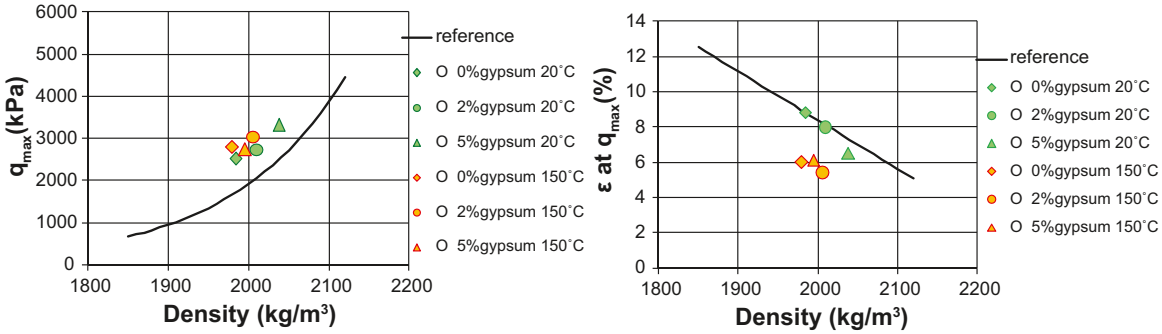

Figure 6-13. *Maximum deviator stress and corresponding strain vs. density for series O.*

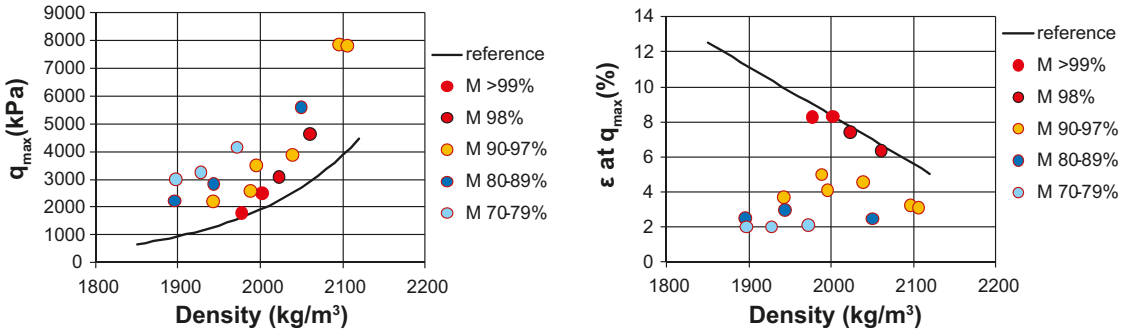

Figure 6-14. *Maximum deviator stress and corresponding strain vs. density for series M.*

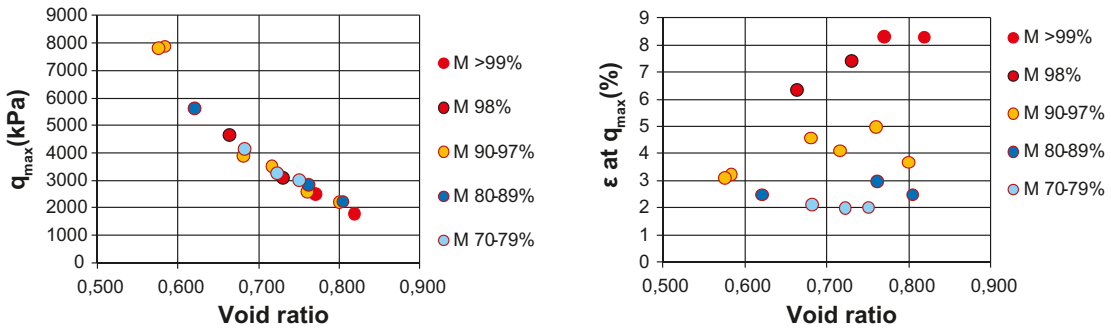

Figure 6-15. *Maximum deviator stress and corresponding strain vs. void ratio from series M.*

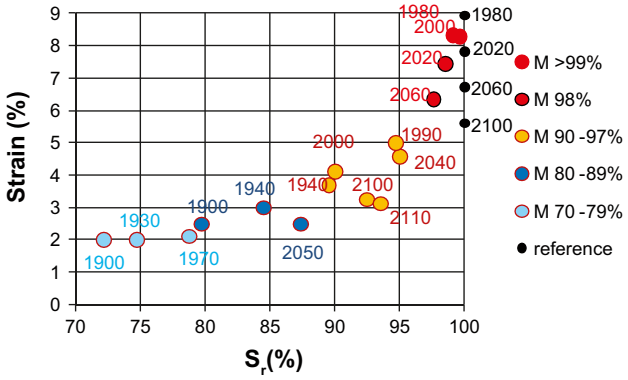

Figure 6-16. *Strain at failure vs. degree of saturation. Bulk densities (kg/m³) are given as data labels.*

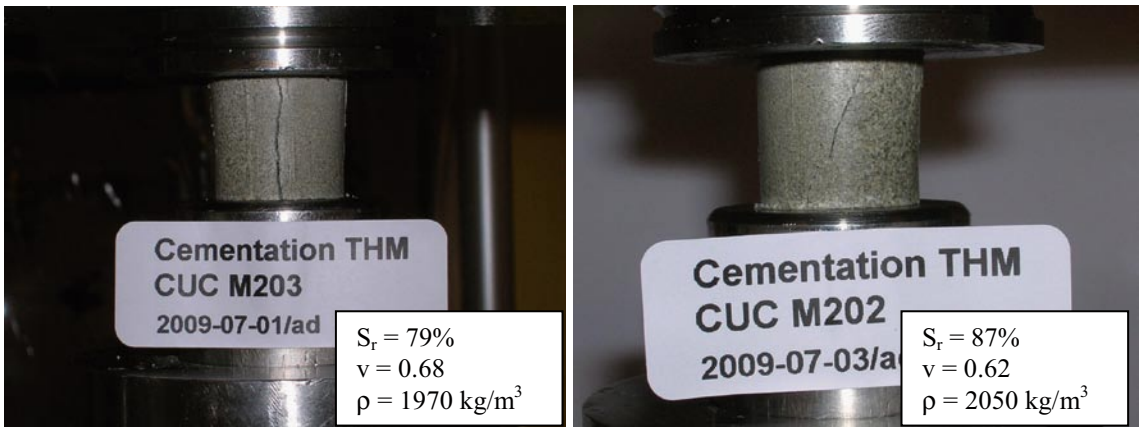

Figure 6-17a. *Inclination of the failure surface at different degree of saturation (79% and 87%) in the test series M.*

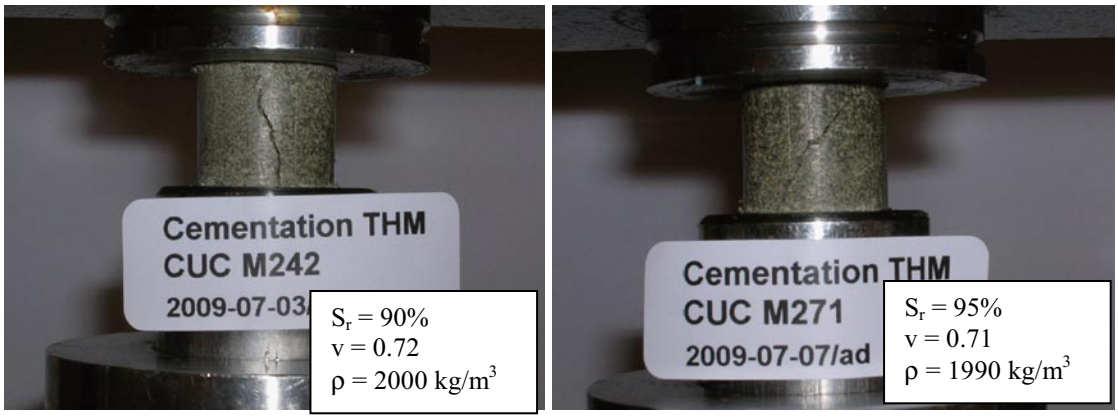

Figure 6-17b. *Inclination of the failure surface at different degree of saturation (90% and 95%) in the test series M.*

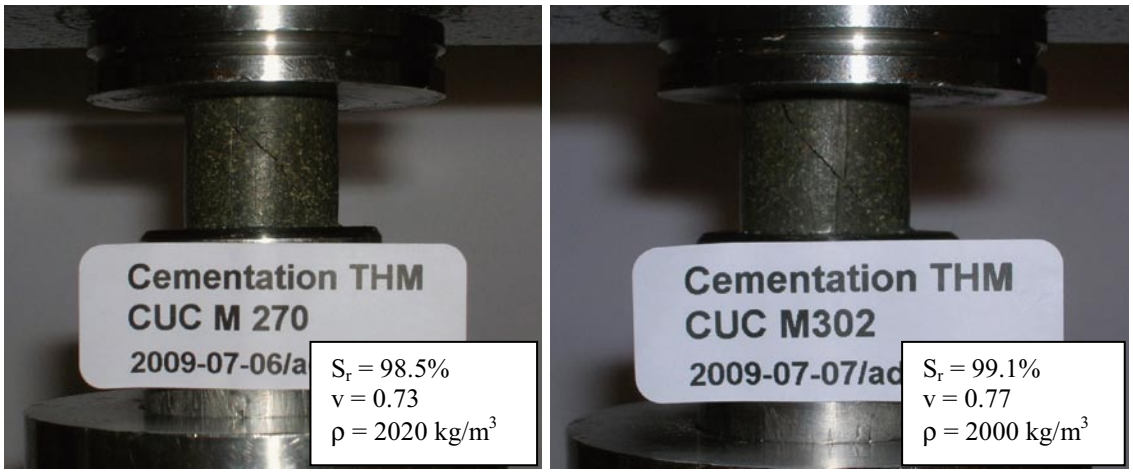

Figure 6-17c. *Inclination of the failure surface at different degree of saturation (98.5% and 99.1%) in the test series M.*

The influence of degree of saturation on strain is large. This is important since the degree of saturation was not always 100% although the specimens were saturated in the saturation device and often also regarded as saturated. In some tests the degree of saturation was as low as 97% after removal from the saturation device. Reduced strain at failure was seen at degree of saturation less than approximately $S_r \leq 97\%$ according to Figure 6-16.

The character of the failure surface was shown to be dependent on the degree of saturation. The ordinary failure surface, with an inclination of 45° to the horizontal plane, was seen only on specimens with $S_r > 98\%$. The inclination increases with decreasing degree of saturation and at $S_r < 90\%$ a vertical failure surface was seen. It should be noted that the character of the failure surface was also dependent on the density.

Thus, small strain at failure was seen on specimens with low degree of saturation. It is uncertain if any *brittle failure* was present among the test results.

6.2.8 Impact of stress anisotropy

An attempt to investigate the influence of anisotropy was made by use of specimens from the ABM field test /Eng et al. 2007/. Sampling for this test series was made in two different directions relative to compaction. The specimens were not saturated in the saturation device and the results are shown in Figure 6-18.

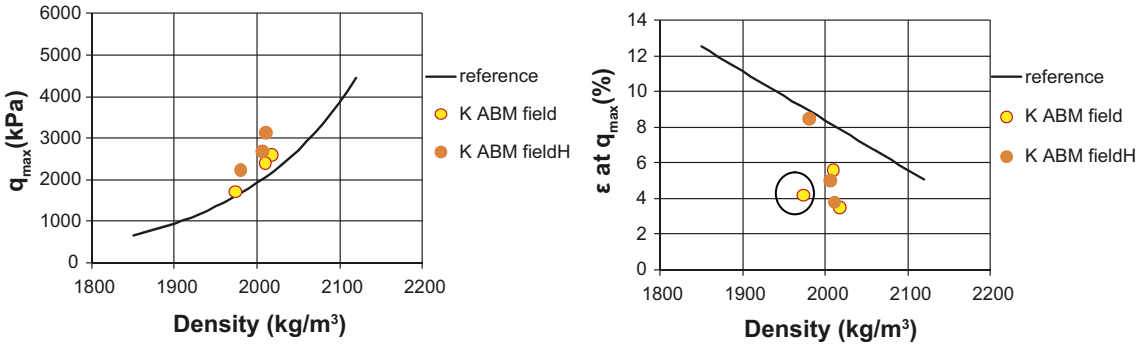

Figure 6-18. *Maximum deviator stress and corresponding strain vs. density for series K.*

There was no significant difference between the results from the three specimens taken in one direction and the three specimens taken in the other direction. However, the horizontal specimens had slightly higher maximum deviator stress. The encircled specimen deviates in strain but had a degree of saturation of 97%. With a higher degree of saturation this specimen should have had a larger strain and also a larger maximum deviator stress. No conclusion about influence of stress anisotropy can be drawn from this series.

6.2.9 Impact of field condition

Results from a limited number of heated and field exposed specimens from the ABM project /Eng et al. 2007/ are shown in Figure 6-19. The results are plotted with results from the heated and field exposed specimens from the LOT project also shown in Figure 1-2. All specimens shown in Figure 6-19 were saturated in the special saturation device.

From both series the results showed that the warmer specimen the lower strains at failure. There was also a trend in both series that the density increased with temperature. The resulting maximum deviator stress showed no significant deviation from the reference line.

In the LOT project the failure at small or reduced strain seen on heated field exposed material in several cases also included abrupt failure behaviour and vertical failure surface /Karnland et al. 2009/. This was not seen on the material from the ABM project, series I. However, *brittle failure* was seen on the ABM specimens taken near the heater and tested in the series K without saturation before shearing.

Thus, small strain at failure was seen on heated field exposed material. *Brittle failure* was seen on the heated field exposed material from the project LOT project but not on the ABM specimens treated in almost the same way.

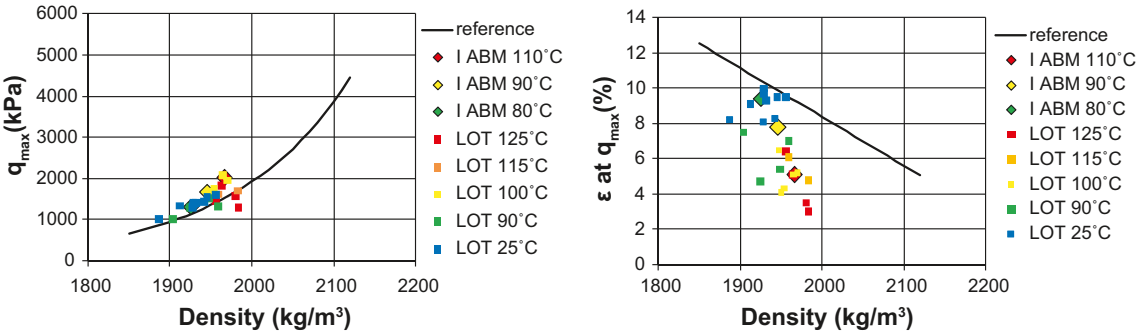

Figure 6-19. *Maximum deviator stress and corresponding strain vs. density for series I. Test results from the LOT series 1 /Karnland et al. 2009/ are also shown.*

6.2.10 Impact of milling and re-compaction

The impact of milling and re-compaction was investigated in a limited series and the results are shown in Figure 6-20. Field exposed material from the warmest part of ABM /Eng et al. 2007/ was used. The results are compared with the results from field exposed material treated in the same way but taken from the LOT project /Karnland et al. 2009/.

By drying, milling and re-compacting the specimens the effect of temperature on strain seemed to disappear and the strains were even larger than the reference. The maximum deviator stress shows no significant deviation from the reference line.

Thus, no reduced strain at failure was seen after drying, milling and re-compaction of heated field exposed material.

6.2.11 Impact of shear rate

Influence of shear rate was investigated by e.g. /Dueck et al. 2010/. From this project specimens with the same density were sheared at different rates ranging from 0.003mm/s to 270 mm/s. From the results in Figure 6-21 it is seen that increased shear rates gives a more smooth behaviour, however not larger strain at failure. In addition, the brittle appearance involved vertical failure surfaces while the more smooth appearance resulting from the high rates involved more ordinary failure surfaces.

From the above the failure can include low strain and have a smooth character if the shearing is fast enough.

Thus, less brittleness is seen when the shearing is very fast.

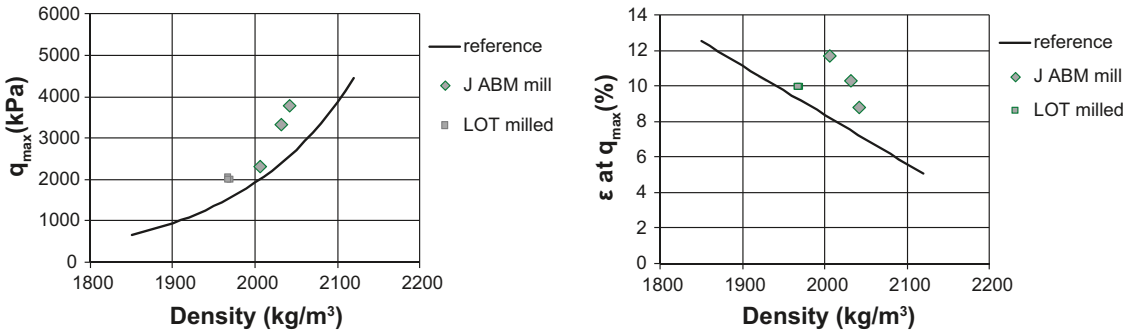

Figure 6-20. *Maximum deviator stress and corresponding strain vs. density for series J. Test results from the LOT series 1 /Karnland et al. 2009/ are also shown.*

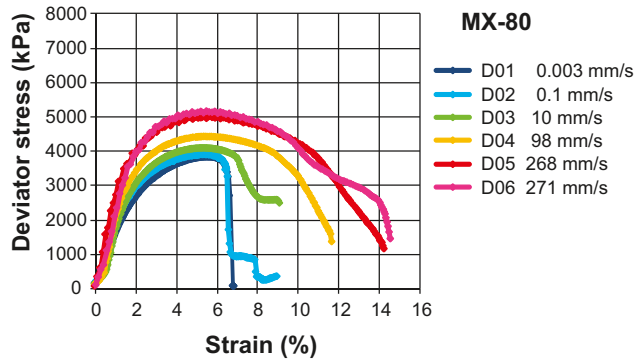

Figure 6-21. *Deviator stress vs. strain at different shearing rates. The material was MX-80 and the density was about 2,040 kg/m³ /Dueck et al. 2010/.*

6.3 Brittle failure, table

In Table 6-1 a compilation of the test results is given and observations of *brittle failure* are marked. In this study the *brittle failure* includes an abrupt decrease in stress after failure, see section 6.1. The *brittle failure* occurred at small strain and often together with a vertical failure surface. There are also conditions where the strain at failure is reduced and these conditions are marked with minus sign in the column marked ε.

Table 6-1. Compilation of test results from tests series A to O and some previous series.

Brittle failure		Maximum deviator stress and corresponding strain[1]		Reasons	Test series
abrupt failure	vertical failure surface	q_{max}	ε		
		0	–	1a. Stress path including $\Delta V \leq 0$ at saturation	A,L
		0	+	1b. Stress path including $\Delta V > 0$ at saturation	A,L,H,D
x	x	+	–	1b. Increased density at room temperature	A, /Karnland et al. 2009/
		0	–	2a. Decreased initial water content	D,H
		0	0	2b Decreased water content at compaction	H
		0	–	2c. More rigid filters	D,H
		0	–	3a. Increased friction on end surfaces	B
		0	0	3b. Minimized time between removal from the sat. device and shearing	/Karnland et al. 2009/, A,B
		+/0	–	4a. Increased temperature and low density	C, E, F,N
x	x	+/0/–	–	4b. Increased temperature and high density	C, E, F,N
		0	0	4c. Increased time of exposure (5h or 24h)	C
		+	0	5. Increased content of Ca^{2+}	E, F, G, /Dueck et al. 2010/
		0	0	6. Increased content of gypsum (0%, 2%, 5%)	O
	x	0	–	7. Decreased degree of saturation at shearing	M
		0	+	9. Milling and re-compaction	J, LOT /Karnland et al. 2009/
		+	0	10. Increased shear rate	/Dueck et al. 2010/

[1] Increased (+) or decreased (–) q_{max} and ε. In case of no difference (0).

7 Discussion and conclusions

7.1 Deviator stress at failure

The following points are important findings from this investigation regarding deviator stress at failure, i.e. maximum deviator stress:

- Higher density gives larger deviator stress at failure.
- A tendency towards increasing deviator stress at failure with increasing temperature is seen on MX-80 and DepCaN. However, the influence of temperature is in the same range as the difference between the two bentonites.
- The initial water content has no influence on the deviator stress at failure.
- The degree of saturation has no influence on the deviator stress at failure for a given void ratio.

7.2 Strain at failure

The following points are important findings from this investigation regarding strain at failure:

- Higher density specimens experienced smaller strain before failure.
- Strain at failure is generally reduced when the specimens have been exposed to increased temperature.
- There is an increase in strain at failure with increasing water content before water saturation.
- The strain at failure is approximately the same for MX-80 and DepCaN at the same density.
- The strain at failure decreases with decreasing degree of saturation.
- There are indications that consolidation decreases the strain at failure while swelling increases the strain at failure, for specimens with the same final density.
- Drying at room temperature, milling and re-saturation restores and even results in larger strain than the reference.

7.3 Brittle failure behaviour

The shear failure is characterized by the maximum deviator stress and the corresponding strain. However, to use strain at failure might be misleading due to its sensitivity to the handling of the specimens before the shearing, e.g. swelling during removal from the saturation device. An alternative to use the value of strain at failure is to classify the failure behaviour. Three categories are shown in Figure 7-1 and are described below:

- Ordinary failure behaviour – large deformation to failure with no or small decrease in stress at failure.
- Failure at reduced strain – smooth failure with obvious maximum at lower strain.
- Brittle failure – abrupt decrease in stress after failure, occurrence of vertical failure surface.

Brittle failure was in this investigation mainly seen on specimens having a density of $\rho \geq 2{,}060$ kg/m^3 or on specimens exposed to high temperature $T \geq 150$°C in the laboratory. The abrupt behaviour seen on unsaturated specimens with densities less than $\rho < 2{,}060$ kg/m^3 occurred on specimens with a degree of saturation less than $S_r < 90\%$. Vertical failure surfaces were seen on these specimens. Brittle failure was also seen in the limited series with purified bentonites. The abrupt behaviour of the failure curve was seen on the purified bentonite WyCa at a density of about 2,000 kg/m^3 but including a vertical failure surface only after heating to 150°C.

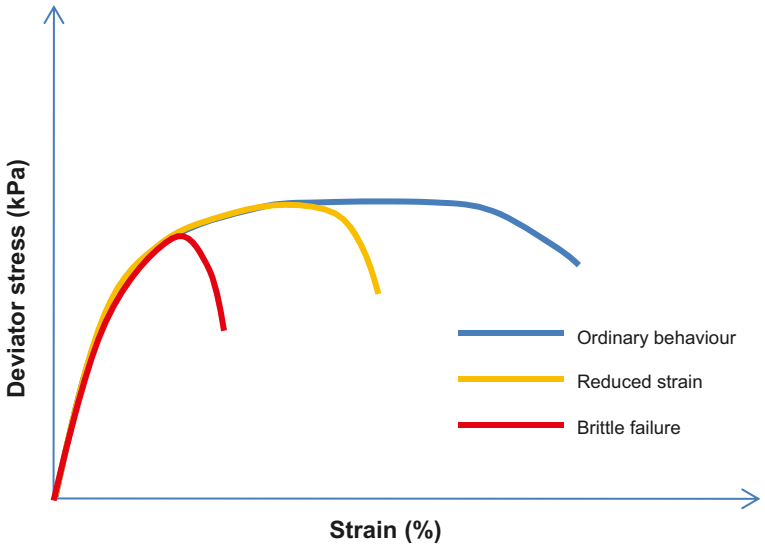

Figure 7-1. *Three categories of failure.*

Failure at reduced strain was seen in this investigation on specimens exposed to $T \geq 150$°C, on specimens having a water content of $w_i = 0\%$ before saturation, on specimens with a final degree of saturation of $S_r \leq 97\%$ and also on one specimen subjected to consolidation. In addition, failure at reduced strain was seen at lower temperatures $T \leq 150$°C on laboratory heated MX-80 specimens /Karnland et al. 2009/.

It was shown that high rate of shear influenced the strain and another mode of failure seemed to occur /Dueck et al. 2010/. The brittle failure on high density specimens tested at the normal rate was exchanged for a smooth behaviour with reduced strain or even ordinary failure behaviour at high rate testing.

Brittle failures were seen on specimens exposed to warm field conditions in the LOT project including abrupt failure behaviour and in several cases also vertical failure surfaces. This behaviour cannot be easily explained by the test results from the present investigation since the density and the maximum temperature of the field exposed material were both lower than required for this behaviour according to the laboratory heated specimens. In addition, the field exposed specimens had a degree of saturation larger than 90% when tested.

7.4 General conclusions from this study

Brittle failure and reduced strain were noticed in the heated field exposed material in the LOT project. Similar behaviour was also observed in the present short term laboratory tests. However, the specimens in the present study showing this behaviour had higher density, lower degree of saturation or were exposed to higher temperatures than the field exposed specimens.

Important observations are that the influence of temperature seen in the present study occurred already after a couple of hours of exposure and that milling and re-compaction after heating restored the original failure behaviour. Further, the influence of temperature on the maximum stress at failure was in the same range as the difference between the tested bentonites.

References

Börgesson L, Johannesson L-E, Sandén T, Hernelind J, 1995. Modelling of the physical behaviour of water saturated clay barriers. Laboratory tests, material models and finite element application. SKB TR-95-20, Svensk Kärnbränslehantering AB.

Börgesson L, Johannesson L-E, Hernelind J, 2004. Earthquake induced rock shear through a deposition hole. Effect on the canister and the buffer. SKB TR-04-02, Svensk Kärnbränslehantering AB.

Dueck A, Börgesson L, Johannesson L-E, 2010. Stress strain relation of bentonite at undrained shear. Laboratory tests to investigate the influence of material composition and test technique. SKB TR-10-32, Svensk Kärnbränslehantering AB.

Eng A, Nilsson U, Svensson D, 2007. Äspö Hard Rock Laboratory; Alternative Buffer Materials, Installation report. SKB IPR-07-15, Svensk Kärnbränslehantering AB.

Karnland O, Olsson S, Nilsson U, 2006. Mineralogy and sealing properties of various bentonites and smectite-rich clay mateials. SKB TR-06-30, Svensk Kärnbränslehantering AB.

Karnland O, Olsson S, Dueck A, Birgersson M, Nilsson U, Hernan-Håkansson T, Pedersen K, Nilsson S, Eriksen T, Rosborg B, 2009. Long term test of buffer material at the Äspö Hard Rock Laboratory, LOT project. Final report on the A2 test parcel. SKB TR-09-29, Svensk Kärnbränslehantering AB.

Appendix 1

Preparation of specimens to test series L

Two specimens were prepared in oedometer devices with a constant diameter of 20 mm. The movable pistons of the oedometer devices were adjusted in steps to change the height of the specimens. The axial stress and the change in height were measured during the preparation.

The objective of the preparation was to end up with two specimens with the same height of 20 mm and different stress paths and final stresses. The specimen subjected to compression had an initial height of 24.5 mm and the specimen allowed to swell had an initial height of 18.4 mm. The measured axial stresses and heights are shown in Figures A1-1 and A1-2 where the consolidation and swelling are denoted by black and red dots, respectively.

From oedometer tests reported by /Börgesson et al. 1995/ the stress state of the specimen SwPr1b is more or less isotropic while the stress state of specimen SwPr1a is anisotropic with the maximum principal stress in the vertical direction. The mean stress is thus assumed to be higher of the specimen SwPr1a than of SwPr1b.

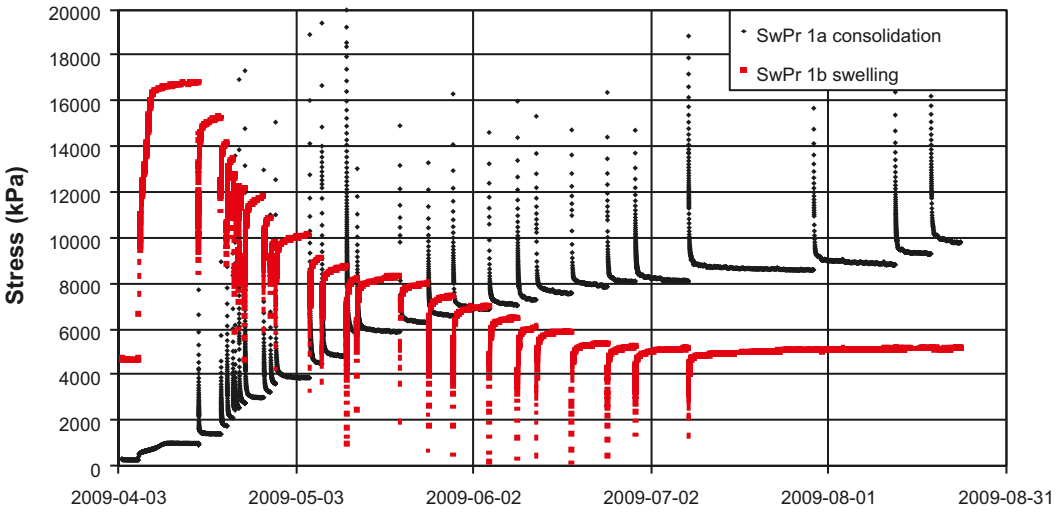

Figure A1-1. *Measured axial stresses during preparation of two specimens to the test series L.*

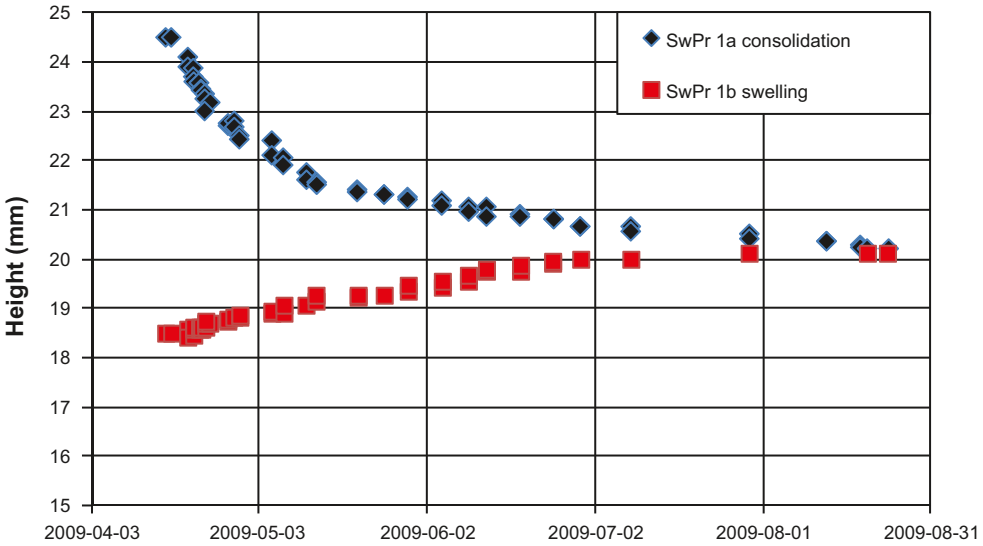

Figure A1-2. *Measured height of two specimens during preparation of two specimens to the test series L.*